

CHANGES IN RICE KERNEL AND STARCH DURING PARBOILING PROCESS

by

SICHAYA SITTIPOD

B.S., Kasetsart University, Thailand, 2010

A THESIS

submitted in partial fulfillment of the requirements for the degree

MASTER OF SCIENCE

Department of Grain Science & Industry
College of Agriculture

KANSAS STATE UNIVERSITY
Manhattan, Kansas

2014

Approved by:

Major Professor
Yong-Cheng Shi

Copyright

SICHAYA SITTIPOD

2014

Abstract

The objective of this study was to systematically understand the changes of rice during the parboiling process. Isolated rice starch, milled rice and paddy rice kernels of the same variety (18% amylose) were examined after steeping at temperatures (60-75 °C) below and above the onset of rice starch gelatinization temperature for different durations in 66.7% water. Changes in gelatinization temperatures were greater for isolated starch >> milled rice > paddy rice. Annealing above samples' original T_0 caused partial gelatinization, loss of crystallinity, and birefringence as determined by X-ray diffraction (XRD), differential scanning calorimetry (DSC), and light microscopy. However, starch granules in milled rice and paddy rice, which were surrounded by non-starch components, maintained their granule integrity. Scanning electron microscopy (SEM) revealed morphological differences between starch granules within native and steeped rice kernels. Steeped kernels had denser structures than native kernels, as determined by high resolution X-ray microtomography. Rice starch granules and kernel characteristics were altered significantly during steeping and changes in isolated starch differed from those inside the rice kernels. To study the changes during the steaming process, the morphology of the rice kernel and starch granules within the kernel were examined immediately after heating at 110°C for 20 min. Starch was completely gelatinized as determined by DSC and XRD, indicating the disruption of all short-range crystallinity of starch in parboiled rice. However, SEM showed intact starch granules and light microscopic images showed starch granules embedded in the rice kernel. Interestingly, these granules displayed Maltese cross patterns. For the first time, we demonstrated that starch granules were birefringent and showed the Maltese cross but were not crystalline.

Table of Contents

Table of Contents	iv
List of Figures	vi
List of Tables	viii
Acknowledgements.....	ix
Dedication	x
Chapter 1 - Changes in rice kernels and starch during steeping in the parboiling process.....	1
Abstract.....	1
Introduction.....	2
Materials and methods	5
Materials	5
Isolation of starch.....	5
Composition analysis	5
Annealing.....	6
Kernel water absorption.....	6
Granule particle size.....	7
Swelling power & solubility	7
Differential scanning calorimetry	7
X-ray diffraction	8
Light microscopy	8
Scanning electron microscopy	9
X-ray microtomography.....	9
Statistical analysis.....	10
Results and discussion	11
Composition of rice kernel and starch	11
Water absorption.....	11
Thermal properties and crystallinity in annealed rice of different forms	12
Morphology of annealed starches and rice kernels.....	14
Swelling and solubility properties of annealed rice starch and flour.....	16
Conclusions.....	17

References.....	18
Chapter 2 - Changes in morphology of starch in parboiled rice kernels	36
Abstract.....	36
Introduction.....	37
Materials and methods	38
Materials	38
Parboiling of rice.....	38
Kernel size determination	39
Light microscopy	39
Differential scanning calorimeter	39
X-ray diffraction	40
Scanning electron microscopy	40
Statistical analysis	40
Results and discussion	41
Thermal and crystalline properties of fresh parboiled rice	41
Morphological structure of parboiled rice	44
Conclusions.....	51
Reference	52
Appendix A.....	54
Detailed procedure for using oil immersion lens	54
Appendix B.....	55
Detailed procedure for isolating rice starch	55
Appendix C.....	58
Detailed procedure for calculating starch relative crystallinity (Microsoft excel method).....	58
Appendix D.....	61
Cryosectioning	61

List of Figures

Figure 1-1 Water absorption of steeped (annealed) paddy, milled rice kernels and isolated starch steeped at 60°C (A) and 70°C (B).	23
Figure 1-2 Onset gelatinization temperature (1), increase in T_o (2), and enthalpy (3) of rice samples annealed at 60°C (A), 65°C (B), 70°C (C), and 75°C (D) up to 16h. (-◆- isolated starch, -■- milled rice, -▲- paddy rice)	25
Figure 1-3 Increase in onset gelatinization temperature (ΔT_o) of 16h annealed starches from different rice sources and annealing temperatures. (-◆- isolated starch, -■- isolated starch from milled flour, -▲- isolated starch from paddy flour)	26
Figure 1-4 X-ray diffractograms of samples annealed at 75° for 16h. Isolated starch and annealed isolated starch (A), native milled flour, annealed milled flour, and isolated starch from annealed milled flour (B), native paddy flour, annealed paddy flour, and isolated starch from annealed paddy flour (C) (top to bottom curve, respectively). The values next to curve are degree of crystallinity.....	27
Figure 1-5 Photomicrographs of 16h annealed starches: native (A), 60°C (B), 65°C (C), 70°C (D), 75°C (E) and starch isolated from annealed milled kernel at 75°C (F) and annealed paddy kernel at 75°C (F) at viewed under bright field (1) and polarized light (2) . (Scale bar = 10 μ m).....	29
Figure 1-6 SEM cross-sections of native and 70°C 4h annealed paddy rice kernels at the interior (A-F) and peripheral regions (G-J) and at different magnifications.	31
Figure 1-7 Rice kernel morphology was measured by X-ray microtomograph. NR= Native rice kernel, AR= Rice kernel annealed at 70°C for 16h. X-ray shadow (raw) images of rice kernels taken at different incremental angles (A). Expanded images for different parts of a rice 2-D sliced image (B). Density distribution of within kernels (C). 2-D crossections images from different parts of kernels (D). The slice number reflects the position of the kernel. The higher the number, the closer to the tip of the kernel.	33
Figure 1-8 Swelling power (1) and solubility (2) of native and annealed starches and milled flour tested at 60°C (A), 75°C (B), and 90°C (C).	34
Figure 1-9 SEM of native rice starch (A), rice starch annealed at 70°C for 16h (B), and rice starch annealed at 75°C for 16h (C). (Scale bar = 10 μ m)	35

Figure 2-1 DSC thermogram of native rice flour- first scan (A1); native rice flour- second scan (A2); commercial parboiled rice (B); aged parboiled rice flour (C); and fresh parboiled rice flour (D).	42
Figure 2-2 XRD diffractogram of native starch (A), commercial parboiled rice flour (B), aged parboiled rice flour (C), and fresh parboiled rice flour (D).	44
Figure 2-3 SEM cross-sections of native and parboiled rice kernels at the interior	47
Figure 2-4 Photomicrograph of native rice starch under bright field and polarized light at x100 oil immersion lens. (Scale bar = 10 μ m).....	48
Figure 2-5. Photomicrographs of fresh parboiled rice flour (A-D) under (1) bright field and (2) polarized light at 40x objective. (Scale bar = 10 μ m).....	48
Figure 2-6 Microtome longitudinal section of parboiled rice kernel viewed under bright field microscope. Note intact cell wall (ICW), disrupted cell wall (DCW) and crack in the starchy endosperm as indicated with arrow. (Scale bar = 20 μ m)	49
Figure 2-7 Microtome longitudinal section of parboiled rice kernel viewed under dark field microscope. Arrow indicates area with Maltese Cross.	50

List of Tables

Table 1-1 Amylose, starch, protein and ash content of rice samples used in annealing process .	21
Table 1-2 Particle size of rice starch steeped (annealed) at different temperatures	22
Table 2-1 Kernel moisture content and size	45

Acknowledgements

I would like to give special thanks to:

- My advisor, Dr. Shi who has given me direction in my work and dedicated his time in helping me learn and grow professionally
- Dr. Seib for his helpful advice and suggestions
- Dr. Dogan for being on my committee member and allowing me to use her laboratory
- Dr. Sun for being my committee member and allowing me to use her laboratory
- Dr. Faubion and Mr. Moore for allowing me to use their laboratory
- Ron Stevens for his help in preparing my samples in the milling lab
- Bruce Ramundo for his help with using the auto clave for parboiling
- Joel Sanneman for his help with kernel microtome sectioning
- All my lab mates and postdocs for supporting me throughout the entire process
- The Royal Princess Sirinthon scholarship foundation for financially supporting me through my education

Dedication

I dedicate this to my parents for their love and support. Thank you for encouraging me to push myself and to never give up.

Chapter 1 - Changes in rice kernels and starch during steeping in the parboiling process

Abstract

Isolated rice starch, milled rice and paddy rice kernels of the same variety (18% amylose) were examined after steeping at temperatures (60-75 °C) below and above the onset of rice starch gelatinization temperature for different durations in 66.7% water. Changes in gelatinization temperatures were greater for isolated starch >> milled rice > paddy rice. Annealing above samples' original T_0 caused partial gelatinization, loss of crystallinity, and birefringence as determined by X-ray diffraction (XRD), differential scanning calorimetry (DSC), and light microscopy. However, starch granules in milled rice and paddy rice, which were surrounded by non-starch components, maintained their granule integrity. Scanning electron microscopy (SEM) revealed morphological differences between starch granules within native and steeped rice kernels. Steeped kernels had denser structures than native kernels, as determined by high resolution X-ray microtomography. Rice starch granules and kernel characteristics were altered significantly during steeping and changes in isolated starch differed from those inside the rice kernels.

Introduction

Parboiling is a three-step hydrothermal process involving the soaking, heating and drying of rice. If performed properly, the process can effectively change physical (e.g. resistant to breakage) and textural characteristics as well as improve nutritional values (Bhattacharya, 2004, Buggenhout et al., 2013). Parboiling conditions have been shown to affect the physicochemical properties of rice such as color formation via Maillard reactions (Lamberts et al., 2006a, Lamberts et al., 2006b) and affect cooked rice texture due to different polymorphic forms of starch: residual starch, re-associated starch, and amylose-lipid complexes, as suggested by Ong and Blanshard (1995). The extent of Vh –type crystallite formation via amylose-lipid complexes has been found to be highly dependent on the moisture content of the kernel, moisture distribution within the kernel, steaming temperature (Derycke et al., 2005) and rice variety based on starch gelatinization onset temperature (Biliaderis et al., 1993). The extent and level of formations of retrograded B-type crystallites originating from crystalline amylopectin and crystalline amylose greatly depend on the parboiling condition and the level of free amylose (Lamberts et al., 2009) .

Kernel steeping is necessary to obtain at least 30% moisture content required for complete gelatinization upon steaming. Miah et al. (2002a, 2002b) studied milling properties and the degree of starch gelatinization of parboiled rice that used hot-soaking temperatures and found that accelerated water penetration into the kernel helped improve the quality of subsequent parboiled rice kernels and the efficiency of parboiling. Because starch makes up more than 80% of a rice kernel, it is important to understand not only how the kernel alters, but also how the starch changes during soaking. When starch is heated in excess amounts of water at a temperature slightly below its gelatinization temperature for a relatively long period, it

undergoes several physiochemical changes as a consequence of annealing as first demonstrated by Gough and Pybus (1971). This process has been known to increase gelatinization temperature, decrease swelling power, and alter pasting properties of starches. Many researchers have studied annealing effects on rice starch (Shi, 2008, Tester & Morrison, 1990a, Tester & Morrison, 1990b). These studies determined annealing of rice in isolated starch form, but the changes in starch when annealed as whole kernels have not been studied.

Non-starch components in rice kernels and integrity of the whole kernel may affect the starch in rice kernels during the steeping step of the parboiling process. Protein, which makes up around 7% of the entire grain, is the second largest component in rice after starch. Protein has been known to contribute to the gelatinization and pasting properties of rice flour (Hamaker & Griffin, 1990). The removal of proteins by buffer or enzyme treatments tends to decrease the gelatinization temperature of flour (Marshall et al., 1990) and increase enthalpy compared to native starch (Zhu et al., 2010). Disulfide bonds of proteins restrict starch from swelling, and disrupting with subject to shear (Hamaker & Griffin, 1993). Without these proteins, starch granules break more easily under high shear and swell more under low shear, because intact proteins provide protection under high shear and act as barriers that restrict swelling under low shear. Zhu et al. (2010) also studied the relationship between starches of waxy rice varieties to their flours and found that after destroying disulfide bonds with DL-dithiothreitol, starch becomes more exposed and susceptible to alpha amylase degradation, depending on the rice variety.

Lipids and waxes also contribute to rice's native barrier. Brown rice is higher in wax content than white rice and has a lower rate of water absorption, which explains why a higher degree of milling and lipid extraction samples have a lower gelatinization peak temperature (T_p)

(Champagne et al., 1990). Similarly, Bello et al. (2004) studied the effects of bran level and hull on the rate of kernel water absorption, and found that the water diffusivity of white rice was higher than that of brown rice, which was higher than that of paddy rice. These authors concluded that the hull and bran fractions provided a diffusion barrier to water and reduced solid leaching. (Normand & Marshall, 1989) also noted the impact of kernel integrity on gelatinization, observing that, producing flour destroys natural barriers, making starch granules more accessible to water and thus lowering gelatinization temperatures.

We hypothesize that the differences in water absorption due to physical barriers would cause different annealing effects on starch granules in rice kernels than in flour or isolated starch. In this study, using thermal and microscopic techniques, we examined changes in isolated rice starch, milled rice and paddy rice kernels of the same long grain variety during steeping at 60-75°C. The starting materials represent three different physical forms with different morphologies and physical barriers. Our goal was to understand the effects of annealing on the changes of rice kernels during the steeping process of parboiling.

Materials and methods

Materials

Long-grain paddy rice was obtained from Mars Food US, Llc. (Los Angeles, CA). Foreign matter was removed by sifting through 10-mesh and 16-mesh standard test sieves (Fisher Scientific, Pittsburgh, PA) and dehulled with a McGill Sheller (McGill Inc., Houston, TX). Bran was removed using a One-Pass Rice Pearler (Model No. 66939396, Satake, Tokyo, Japan) for 30 seconds to obtain milled rice kernels (DM= 15%), which were then ground to obtain milled rice flour. Chemicals were analytical grade.

Isolation of starch

Rice starch isolation was based on an alkaline-protease method (Lumdubwong & Seib, 2000) with slight modifications (Zhu et al., 2011) on milled rice kernels. [**Appendix B** provides the details procedure.]

Composition analysis

Amylose content was determined by a modified ConA Method developed by Yun and Matheson (1990) and total starch was determined by AACC Method 76-13 (AACC International, 2000), each with an assay kit from Megazyme International Ltd. (Wicklow, Ireland). Moisture content was measured according to AACC Air Oven Method 44-19 (AACC International, 2000) in a convention oven (Model 160DM Thelco, Precision Scientific, Chicago, IL) at 135°C for 2 h. Crude protein content was determined by the nitrogen combustion method using a Nitrogen Determinator (LECO FP-528, St. Joseph, MI) according to AOAC standard method 990.03 (AOAC International, 1995). Nitrogen values (N) were converted to protein content using an N x 5.95 conversion factor. Total ash was based on AACC international method 946.05. All tests were done in duplicate.

Annealing

Thirty grams each of paddy rice kernels, milled rice kernels, and isolated starch were placed in glass jars filled with 66.7% distilled water and placed in a water bath (reciprocal shaking bath model 50: Precision Scientific, Chicago, IL) kept at constant temperature of 60, 65, 70 and 75 °C. The jars were removed at 0.5, 1, 2, 4, 8, and 16 h time intervals. Paddy and milled rice were then drained of excess water and air dried until the moisture content was about 12%. Isolated starch slurrie annealed at 60-70 °C were centrifuged (Beckman, model J2-21) at 5,000g for 15 min, and the starch was air-dried at 30 °C for 24 h. The isolated starch slurry annealed at 75 °C was added to absolute ethanol (200ml) with agitation. The mixture was centrifuged at 10,000 rpm for 15 min and washed with acetone once. The starch was then dried using a vacuum pump equipped with a condenser system to trap the acetone solvent. Dried starch was then hand ground into fine powder using a mortar and pestle. Dried kernels were ground into flour using a coffee grinder (Model CM08, Hamilton Beach Brands, Inc., Richman, VA). Annealed paddy rice flour refers to flour from steeped paddy rice kernels. Annealed milled rice flour refers to flour from steeped milled rice kernels.

Kernel water absorption

Steeped paddy rice and milled rice were drained and lightly blotted with filter paper to remove excess water before being placed in a conventional oven (Model 160DM Thelco, Precision Scientific, Chicago, IL) at 105°C for 24h to determine moisture content. Tests were done in duplicate.

Granule particle size

Particle size distribution of starches was measured using a Laser Scattering Particle Size Distribution Analyzer (Model LA-910, Horiba, Ltd., Japan). Starch (~10 mg) was suspended in 2 ml of distilled water and slowly introduced into the machine's water reservoir until the light transmittance requirement reached around 85%. The suspension was sonicated for 60 seconds to prevent agglomeration before analysis. The calculated diameter (μm) was based on particle volume and the assumption that all particles were spherical in shape. Three replicates were done per sample.

Swelling power & solubility

A suspension was prepared with 1% (w/v) of starch or flour in 45-ml centrifuge tubes with distilled water. Tubes were immersed in the water bath at 60, 75, and 90 °C for 30 min and shaken every 5 min during heating. Tubes were then removed, cooled and centrifuged at 3000g for 15 min. Supernatant was decanted onto glass Petri dishes of predetermined weight and dried at 100°C overnight. The weight of the remaining wet sediment paste in the centrifuge tubes was determined. Swelling power was calculated as grams of the sediment paste per gram of dry starch weight in the wet sediment. The weight of dried solids in supernatant was used to calculate solubility as grams of solids in supernatant per gram of starch weight in flour.

Differential scanning calorimetry

Thermal properties were determined in duplicate using DSC (Q100, TA Instruments, New Castle, DE). Approximately 9 mg of starch were accurately weighed into a high-volume stainless steel DSC pan. Distilled water was added to obtain a starch to water ratio of 1:2 (w/w).

The sample pans were hermetically sealed and heated from 10 °C to 120 °C at the rate of 10 °C/min. The transition temperatures reported were the gelatinization onset (T_o), peak (T_p), and conclusion (T_c) temperatures. The enthalpy of gelatinization (ΔH) was calculated using Universal Analysis (TA Instruments) and normalized to the dry weight of the sample.

X-ray diffraction

X-ray diffraction was conducted with a X-ray diffractometer (APD 3520, Philips, Eindhoven, Netherlands) with Cu $K\alpha$ radiation at 35 kV and 20 mA, a theta-compensating slit, and a diffracted beam monochromator. The moisture of all samples was adjusted to about 20% in a sealed dessicator (100% relative humidity) at room temperature for 48 h prior to analysis. The diffractograms were recorded from 3° to 30° (2θ). Relative crystallinity was estimated by calculating the ratio of the peak areas to the total diffractogram area. [Detailed calculation methods can be found in **Appendix C.**]

Light microscopy

Flour and starch samples were examined under bright field and polarized light using an Olympus BX51 microscope (Olympus America Inc., Melville, NY). Samples were prepared by dispersing approximately 10 mg into 2 ml of 75% glycerol-water solution then transferring a single drop to a glass slide. Samples were viewed through a coverslip for images viewed at 40x objective. Immersion oil was used for samples viewed at 100x objective. [**Appendix A** provides step-by-step details.] Images were captured and analyzed using SPOT Insight camera and SPOT ADVANCE software (Diagnostic Instruments Inc., Sterling Heights, MI).

Scanning electron microscopy

Rice kernel morphology was examined by a SEM (S-3500N, Hitachi Science Systems, Ltd, Japan) at an accelerating potential of 5 kV using an X-ray Detector-Link Pentafet 7021 (Oxford Instruments Microanalysis Limited, Bucks, England). Each grain was manually fractured at the middle and a blade was used to trim off the bottom end. The fractured cross-sections of the kernel were mounted, face up on an aluminum stud using double-sided adhesive tape. They were then sputter-coated with gold palladium (60:40 ratio) 3 times for 20 seconds under vacuum with a Desk II Sputter/Etch Unit (Denton Vacuum, LLC, Moorestown, NJ) before viewing.

X-ray microtomography

Rice kernels were scanned using a high-resolution desktop XMT imaging system (Model 1072, Skyscan, Aartselaar, Belgium), as according to (Zhu et al., 2012) with slight modifications. The XMT consists of a microfocus sealed X-ray tube with a spot size of 5 mm operating at a voltage/current of 46 kV/75 mA, a rotatable stage, and a 12-bit, cooled CCD-camera (1024 x1024 pixels). Rice kernels were positioned on the specimen stage which rotated around the axis perpendicular to the beam direction, then scanned. Areas differing in density within a kernel resulted in differences in X-ray attenuation. Samples were scanned at a magnification of x 55. During image acquisition process, the samples were rotated by a total angle of 180°. The X-ray images were obtained every 1.8° of rotation with an exposure time of 1.2 seconds for each step, resulting in approximately 200 shadow images per sample. The total scanning time for each sample was approximately 30 min. After scanning, shadow images for each kernel were loaded into NRecon reconstruction software (V1.5.1, SkyScan, Belgium). This software graphically combines the images into a 3-D object from which 2-D cross-sectional images can be taken.

Reconstructions of the grayscale frequency scatter plot were set at a dynamic range of 0.03-0.10. After the 3-D structure was constructed, virtual cuts or slices of the kernel were made, allowing accurate analysis of internal structures from various angles. The software enables calculation of numerical data from the morphology of sample structures. Quantitative analysis of XMT images involves several steps: image reconstruction (3-D virtual model generation), creation of axial images (cross-sectional slices), defining the region of interest (ROI) and the volume of interest (VOI), thresholding (creating binary images), despeckling, and finally calculation of structural properties. Analysis of 3-D rice kernels was conducted with CTAn processing and analysis software (v. 1.7). A total of 975 reconstructed images were entered. A rectangular selection was then interpolated by the software across all of the selected image layers, cropping them to create a 3-D VOI. Selected regions of interest were then saved as independent data sets. Cropping the original sample cross-sectional images to selected ROIs reduces the file size of sample images and greatly lowers the burden of sample processing on the computer system. Algorithms developed by CT-Analyser (version 1.4, SkyScan) were used to extract microstructural features of rice kernels. Various morphometric parameters such as void volume, structure separation (average cell size), cell size distribution, structure thickness (average cell wall thickness) and cell wall thickness distribution, fragmentation index, and structure model index were calculated in 3-D. In this study, void fraction was calculated by void volume divided by total volume of the ROI.

Statistical analysis

Data were analyzed using the variance (ANOVA) procedure with the Duncan multiple range test using SAS version 9.1 (SAS Institute, Inc., Cary, NC). Mean values of replicates and standard deviations were reported.

Results and discussion

Composition of rice kernel and starch

Compositions of flours and isolated starch are shown in Table 1. Isolated starch had very low levels of protein (0.3%) and ash (0.03%), whereas milled rice and paddy rice flour had 6.9% and 8.1% protein, respectively. The SEM photomicrograph presents the three forms of rice used for the annealing treatment. Isolated starch represents starch granules that are free of non-starch components. Milled rice and paddy rice sample represents starch in compound granules and embedded in a protein matrix, differing in bran layer and hull during the steeping process.

Water absorption

Water absorption rates were different among rice starch, milled rice and paddy rice (Fig. 1.1). Isolated starch annealed at 70 °C absorbed up to 65% water whereas milled and paddy rice absorbed approx. 35% water. At the same annealing temperature, the moisture content of starch >> milled \approx paddy, suggesting that water could penetrate more into individual isolated starch granules than into starch granules within the kernel where the starch granules are packed in compact granules and embedded in a protein matrix. Milled kernels also appeared to absorb slightly more water than paddy kernels during initial uptake. Annealing at 70 °C resulted in higher moisture uptake than at 60 °C after the same duration of annealing. Our findings agree with Horigane et al. (2006), who used magnetic resonance imaging technology to identify initial water penetration patterns of rice kernels. Milled and brown rice kernels of the same variety differ in penetration pattern due to the physical inhibition of water from the pericarp of brown rice samples.

Thermal properties and crystallinity in annealed rice of different forms

Changes in thermal properties upon annealing are clearly dependent on the form of the starting material. Fig. 1.2 shows gelatinization onset temperatures (T_o), increases in T_o (ΔT_o), and enthalpy values of annealed samples (left to right). Original T_o of native isolated rice starch, milled rice flour, and paddy rice flour were 73.5, 74.7 and 75.1 °C respectively. At all four annealing temperatures, T_o increased with increasing annealing time as shown in previous studies (Lan et al., 2008, Waduge et al., 2006). Similarly to the water absorption curve, there was a rapid initial increase in T_o after the first 2h. At any particular annealing temperature, ΔT was generally higher for starch than were for milled and paddy rice flour, which is in agreement with the higher water absorption rate of starch than flour. At 16h, ΔT for starch increased to 2, 4, and 6 °C at 60, 65, and 70 °C respectively and was 14 °C higher than native starch at 75 °C. This significant increase is due to partial gelatinization and the melting of weak crystals with lower T_o as shown through significant enthalpy loss, and perfecting of remaining strong crystals as annealing time increases. It is important to note that ΔT_o of flour samples maintained below 6 °C, even after 16h at 75 °C. The initial enthalpy (ΔH) values were 16 J/g for starch and ~ 10 J/g for milled and paddy rice flours and interestingly, they all remained relatively constant when annealed at 60 -65 °C. These results are similar to the findings of Shi and Seib (1992), who annealed waxy rice starches 6 °C below their original T_o and found that even though T_o increased and gelatinization peak narrowed, there was little change in ΔH . It must be noted, however, that starches of the same variety but grown at different temperatures may contain crystallites with a different degrees of perfection, in which case the T_o may increase equally, but starches with lower T_o will result in partial or total gelatinization, as studied in six non waxy wheat cultivars (Shi et al., 1994). When starches were annealed at 75 °C, starch enthalpy decreased significantly

within the first hour. However, it is interesting to note that annealing at 70 °C also caused a decrease in starch enthalpy, even though the temperature was still below T_0 . Flour samples maintained enthalpy even at 75 °C which was above starch's original T_0 .

The ΔT_0 of starch isolated from annealed milled rice and annealed paddy rice samples were compared with annealed isolated starch at 16h and are shown in Fig. 1.3. With an increase in annealing temperature, T_0 increases, but changes were significantly less for starch isolated from annealed kernels than from annealed isolated starch. These data support the idea that kernel integrity, i.e. the presence of non-starch components and a tight morphological structure of starch inhibits heat modification of the starch granules. The kernel integrity affects the moisture content gradient of the peripheral layer and interior layer (Swamy & Bhattacharya, 2009), which would affect phase transition. During short steeping durations, interior endosperm layer receive limited water, which then could affect the overall DSC transition temperatures of the sample.

XRD patterns are in agreement with DSC data that heat modification of annealed starches and rice kernels are different. Figs. 1.4(B –C) each presents 3 forms of rice: flour, annealed flour, and its annealed starch counter parts at 75 °C. Native starch displayed a typical A-type crystallinity pattern and had 44.19% crystallinity. Crystallinity of isolated starch from annealed flours were very close to that of native starch crystallinity but isolated starch samples annealed at 75 °C lost the majority of their crystallinity (Fig. 1.4A). This result may be explained using the moisture absorption curve (Fig. 1.1), which shows that starches naturally absorb more water than flour after the same period of time. High moisture and high temperature condition lead to higher molecule mobility and facilitate a shift in the samples' gelatinization to a lower temperature. Because isolated starch from annealed flour and annealed flours were both annealed in kernel form, the flour's crystallinity content were maintained and were similar to each other whereas

starch annealed at 75 °C had a dramatically lower crystallinity content because it had gelatinized during the treatment. Starch granules in flour samples are not modified to the same extent as starch because of moisture content difference between the starch and flour samples during annealing.

Morphology of annealed starches and rice kernels

Photomicrographs under bright field and polarized light (Fig. 1.5A-E) of isolated starch annealed for 16h at different temperatures show the effects of annealing temperature on starch granule morphology and birefringence. After annealing at high temperatures, starches appeared slightly bigger. Starch annealed at 70 °C lost some birefringence due to partial gelatinization (Fig. 1.5D), and starch was highly gelatinized when annealed at 75 °C (Fig. 1.5E). This finding is also in agreement with particle size analysis (Table 1.2), because annealed starch granules swelled more at high temperature in water than native starch granules. Starch annealed 75 °C had the biggest particle size. On the other hand, isolated starch from annealed paddy and milled rice at 75 °C (Fig. 1.5F-G) showed granule integrity. These data also confirm that starch granules taken from annealed flour samples were less altered than annealed starches.

The SEM images (Fig. 1.6) show the morphology of kernels before and after annealing at 70 °C for 4h. Kernel cross-section images of the interior and peripheral layers revealed that starch granules in the interior layer of native rice appear to have sharp polygonal shapes, whereas annealed samples appeared more rounded. Individual starch granules of annealed samples seem to merge together within the compound structure. This finding is in agreement with Swamy and Bhattacharya (2009), who suggested that prolonged soaking seals fissures in rice due to the swelling of starch granules. The appearance of starch granules in the peripheral layer is similar to that of the interior layer except that distinct protein bodies were observed and embedded in

crevices between starch granules. Buggenhout et al. (2013) noted that soaking had some impact, on the extractability of protein, although to a much lesser extent than parboiling. These authors suggested that more severe steeping conditions may have caused differences in grain moisture content and temperature, which led to changes in rice protein conformation that would promote more protein polymerization upon parboiling (Buggenhout et al., 2013). The morphology of our sample supports this idea by showing that annealed proteins appear visually different than native protein.

X-ray microtomography was applied to determine annealed kernels density (Fig.1.7). Fig 1.9A shows X-ray images of a rice kernel taken at 0° , 90° and 180° angles. Fig. 1.7B shows a cross-section layer mid-kernel, which revealed that the density of rice kernel increased after annealing. The density at the center of the kernel was higher compared with the outer portion of the kernel after annealing. The density also became more uniform in each layer from the bottom to the tip of the kernel (Figs. 1.7C-D). An increase in density after soaking was also found by Kashaninejad et al. (2007), who determined kernel density using the pycnometer (toluene displacement) method. Void fractions of the kernels were 58.2% and 59.5% respectively. Although changes in the packing of crystallite remained undetected and void fractions were similar, it is possible that the increase in T_o and crystalline homogeneity may have gradually changed the appearance of starch granules and their compactness within compound granule inside the kernel as shown in our SEM results. Miah et al. (2002a, 2002b) discovered that water that penetrated into the endosperm's void spaces could seal internal fissures of the grain which increased head rice yield.

Swelling and solubility properties of annealed rice starch and flour

Swelling power and solubility tests were performed on milled rice flour and starch at 60 °C, 75 °C and 90 °C. Milled rice flour was chosen because the thermal properties of milled and paddy rice flour are similar. The swelling power of native and annealed samples increased with increasing assay temperature (Fig. 1.8A1, B1, and C1 respectively). When assayed at 60 °C and 75 °C, there were no significant differences between native starch and starch samples annealed below T_o . However, starch annealed at 75 °C (above T_o) had significantly higher swelling power and solubility. Swelling power depends on the water-holding and water binding capacities of starch molecules via hydrogen bonding (Lee & Osman, 1991). Thus swelling power and solubility can be used to determine the extent of starch chain interactions within the amorphous and crystalline regions (Wani et al., 2012). This suggests that granules were weaker, which was observed with the sample's disrupted granules and crystalline structure prior to testing (Fig. 1.4 and Fig. 1.9). Exposed hydroxyl groups of amylose and amylopectin lead to the formation of hydrogen bonds with water (Tester & Karkalas, 1996), which result in increased swelling power and higher solubility of starch (Fig. 1.8A2). Because flour samples' crystallinity were hardly altered after annealing at 75 °C, no significant differences were found in the swelling powers of any of the flour samples, as expected.

The dramatically higher swelling power of starch and flour when tested at 90 °C is in accordance with Tester & Morrison (1990a), who observed multi- phases of swelling power in normal and waxy barley and maize starches based on temperature. Vandeputte et al. (2003) also suggested that for rice starch, the first stage of swelling occurs at 55-85 °C whereas the second stage causes pronounce swelling at 85-120 °C, which is in the range for rice starch gelatinization. There was no significant difference in swelling power among annealed starches (Fig. 1.8C1).

Native and annealed starches had gelatinization conclusion temperatures (T_c) from 83-94 °C, therefore, all the starch samples would have significantly gelatinized by the end of the analysis, so the swelling power of these samples became similar. The low solubility of flour annealed at 75°C reflects that the flour was able to swell greatly but not solubilize as much. In addition, gelatinized matrixes can also form a 3-D network that can hold additional water (Lee & Osman, 1991). The gelatinized flour matrix therefore appears to hold much more water than matrix gelatinized starch alone, based on our data.

Conclusions

Isolated starch absorbed more water than milled and paddy rice when annealed at 60-75°C. The increase in gelatinization temperature was greater for isolated starch >> milled rice > paddy rice. Annealing above the onset gelatinization temperature caused partial gelatinization, loss of crystallinity and birefringence but starch granules in milled and paddy rice maintained granule integrity.

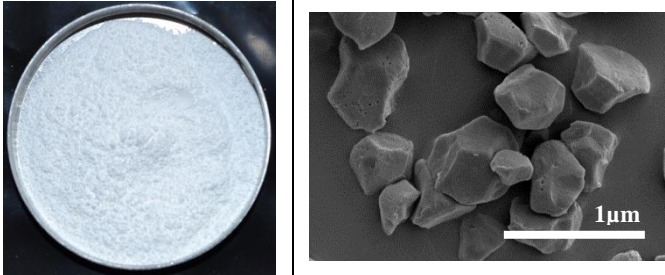
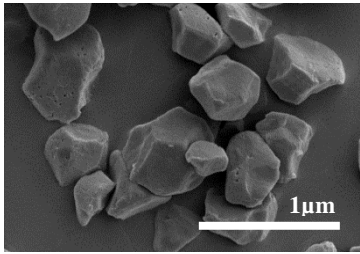

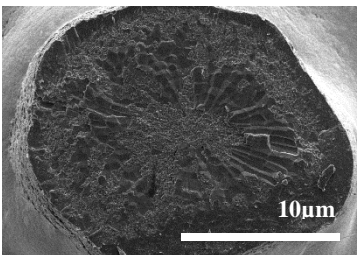

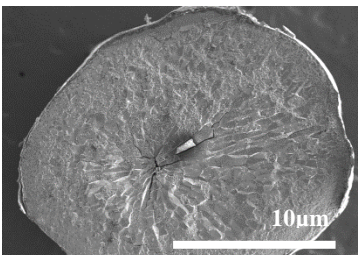
References

- Bello, M., Tolaba, M.P., Suarez, C., 2004. Factors affecting water uptake of rice grain during soaking. *LWT-Food Science and Technology* 37, 811-816.
- Bhattacharya, K.R., 2004. Rice: Chemistry and Technology. In: Champagne, E.T. (Ed.), , 3rd ed. American Association of Cereal Chemists, St. Paul, Minn., pp. 329-404.
- Biliaderis, C.G., Tonogai, J.R., Perez, C.M., Juliano, B.O., 1993. Thermophysical properties of milled rice starch as influenced by variety and parboiling method. *Cereal Chemistry* 70, 512-516.
- Buggenhout, J., Brijs, K., Delcour, J.A., 2013. Impact of processing conditions on the extractability and molecular weight distribution of proteins in brown parboiled rice. *Journal of Cereal Science* 58, 8-14.
- Buggenhout, J., Brijs, K., Delcour, J.A., 2013. Impact of Starch Gelatinization and Kernel Fissuring on the Milling Breakage Susceptibility of Parboiled Brown Rice. *Cereal Chemistry* 90, 490-496.
- Champagne, E., Marshall, W., Goynes, W., 1990. Effects of the degree of milling and lipid removal on starch gelatinization in the brown rice kernel. *Cereal Chemistry* 67, 570-574.
- Derycke, V., Vandeputte, G., Vermeulen, R., De Man, W., Goderis, B., Koch, M., Delcour, J., 2005. Starch gelatinization and amylose–lipid interactions during rice parboiling investigated by temperature resolved wide angle X-ray scattering and differential scanning calorimetry. *Journal of Cereal Science* 42, 334-343.
- Gough, B., Pybus, J., 1971. Effect on the gelatinization temperature of wheat starch granules of prolonged treatment with water at 50 C. *Starch-Stärke* 23, 210-212.
- Hamaker, B.R., Griffin, V.K., 1993. Effect of disulfide bond-containing protein on rice starch gelatinization and pasting. *Cereal Chemistry* 70, 377-380.
- Hamaker, B.R., Griffin, V.K., 1990. Changing the viscoelastic properties of cooked rice through protein disruption. *Cereal Chemistry* 67, 261-264.
- Horigane, A.K., Takahashi, H., Maruyama, S., Ohtsubo, K., Yoshida, M., 2006. Water penetration into rice grains during soaking observed by gradient echo magnetic resonance imaging. *Journal of Cereal Science* 44, 307-316.
- Kashaninejad, M., Maghsoudlou, Y., Rafiee, S., Khomeiri, M., 2007. Study of hydration kinetics and density changes of rice (Tarom Mahali) during hydrothermal processing. *Journal of Food Engineering* 79, 1383-1390.

- Lamberts, L., Bie, E.D., Derycke, V., Veraverbeke, W., De Man, W., Delcour, J., 2006a. Effect of processing conditions on color change of brown and milled parboiled rice. *Cereal Chemistry* 83, 80-85.
- Lamberts, L., Brijs, K., Mohamed, R., Verhelst, N., Delcour, J.A., 2006b. Impact of browning reactions and bran pigments on color of parboiled rice. *Journal of Agricultural and Food Chemistry* 54, 9924-9929.
- Lamberts, L., Gomand, S.V., Derycke, V., Delcour, J.A., 2009. Presence of amylose crystallites in parboiled rice. *Journal of Agricultural and Food Chemistry* 57, 3210-3216.
- Lan, H., Hoover, R., Jayakody, L., Liu, Q., Donner, E., Baga, M., Asare, E., Hucl, P., Chibbar, R., 2008. Impact of annealing on the molecular structure and physicochemical properties of normal, waxy and high amylose bread wheat starches. *Food Chemistry* 111, 663-675.
- Lee, Y., Osman, E.M., 1991. Correlation of morphological changes of rice starch granules with rheological properties during heating in excess water. *Journal of Agricultural Chemistry and biotechnology, Korean* 34, 63-74.
- Lumdubwong, N., Seib, P., 2000. Rice starch isolation by alkaline protease digestion of wet-milled rice flour. *Journal of Cereal Science* 31, 63-74.
- Marshall, W., Normand, F., Goynes, W., 1990. Effects of lipid and protein removal on starch gelatinization in whole grain milled rice. *Cereal Chemistry* 67, 458-463.
- Miah, M., Haque, A., Douglass, M.P., Clarke, B., 2002a. Parboiling of rice. Part I: Effect of hot soaking time on quality of milled rice. *International Journal of Food Science & Technology* 37, 527-537.
- Miah, M., Haque, A., Douglass, M.P., Clarke, B., 2002b. Parboiling of rice. Part II: Effect of hot soaking time on the degree of starch gelatinization. *International Journal of Food Science & Technology* 37, 539-545.
- Normand, F., Marshall, W.E., 1989. Differential scanning calorimetry of whole grain milled rice and milled rice flour. *Cereal Chemistry* 66, 317-320.
- Ong, M.H., Blanshard, J., 1995. The significance of starch polymorphism in commercially produced parboiled rice. *Starch-Stärke* 47, 7-13.
- Shi, Y.-C., 2008. Two-and multi-step annealing of cereal starches in relation to gelatinization. *Journal of Agricultural and Food Chemistry* 56, 1097-1104.
- Shi, Y.-C., 1994. Effects of temperature during grain-filling on starches from six wheat cultivars. *Cereal Chemistry* 71, 369-383.

- Shi, Y.-C., Seib, P.A., Bernardin, J.E., 1992. The structure of four waxy starches related to gelatinization and retrogradation. *Carbohydrate Research* 227, 131-145.
- Swamy, Y., Bhattacharya, K., 2009. Induction and healing of cracks in rice grain during water-soaking of paddy. *Journal of Food Science and Technology (Mysore)* 46, 136-138.
- Tester, R.F., Karkalas, J., 1996. Swelling and gelatinization of oat starches. *Cereal Chemistry* 73, 271-277.
- Tester, R.F., Morrison, W.R., 1990a. Swelling and gelatinization of cereal starches. I. Effects of amylopectin, amylose, and lipids. *Cereal Chemistry* 67, 551-557.
- Tester, R.F., Morrison, W.R., 1990b. Swelling and gelatinization of cereal starches. II. Waxy rice starches. *Cereal Chemistry* 67, 558-563.
- Vandeputte, G., Derycke, V., Geeroms, J., Delcour, J., 2003. Rice starches. II. Structural aspects provide insight into swelling and pasting properties. *Journal of Cereal Science* 38, 53-59.
- Waduge, R., Hoover, R., Vasanthan, T., Gao, J., Li, J., 2006. Effect of annealing on the structure and physicochemical properties of barley starches of varying amylose content. *Food Research International* 39, 59-77.
- Wani, A.A., Singh, P., Shah, M.A., Schweiggert-Weisz, U., Gul, K., Wani, I.A., 2012. Rice Starch Diversity: Effects on Structural, Morphological, Thermal, and Physicochemical Properties—A Review. *Comprehensive Reviews in Food Science and Food Safety* 11, 417-436.
- Yun, S., Matheson, N.K., 1990. Estimation of Amylose Content of Starches after Precipitation of Amylopectin by Concanavalin-A. *Starch-Stärke* 42, 302-305.
- Zhu, L., Dogan, H., Gajula, H., Gu, M., Liu, Q., Shi, Y., 2012. Study of kernel structure of high-amylose and wild-type rice by X-ray microtomography and SEM. *Journal of Cereal Science* 55, 1-5.
- Zhu, L., Liu, Q., Sang, Y., Gu, M., Shi, Y., 2010. Underlying reasons for waxy rice flours having different pasting properties. *Food Chemistry* 120, 94-100.
- Zhu, L., Liu, Q., Wilson, J.D., Gu, M., Shi, Y., 2011. Digestibility and physicochemical properties of rice (*Oryza sativa L.*) flours and starches differing in amylose content. *Carbohydrate Polymers* 86, 1751-1759.

Table 1-1 Amylose, starch, protein and ash content of rice samples used in annealing process

Sample		Composition (%)			
		Amylose content	Starch	Protein	Ash
<p>Isolated rice starch</p> 		18.5± 0.9	97.4±0.02	0.3± 0.02	0.03±0.01
<p>Milled rice</p> 		18.5± 0.9	81.8± 2.6	6.9± 0.03	0.53±0.06
<p>Paddy rice</p> 		18.5± 0.9*	81.7±0.02*	8.1± 0.2*	1.13±0.1*

*Determined after removing hull

Table 1-2 Particle size of rice starch steeped (annealed) at different temperatures

Annealing Temperature (°C)	Volumetric Diameter (µm)*
Control	5.17±0.06 c
60	5.19±0.03 c
65	5.23 ±0.05 c
70	6.57±0.06 b
75	12.39±0.06 a

^a Values in the same column followed by the same letter are not significantly different ($P < 0.05$)

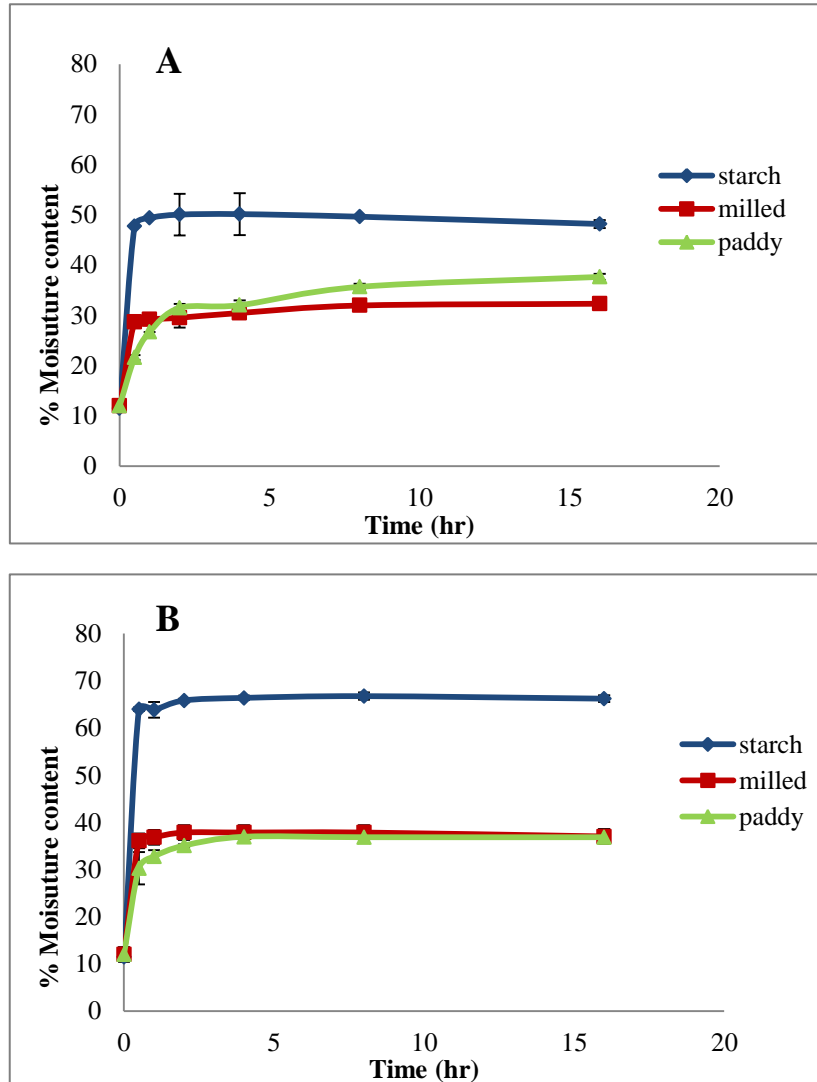
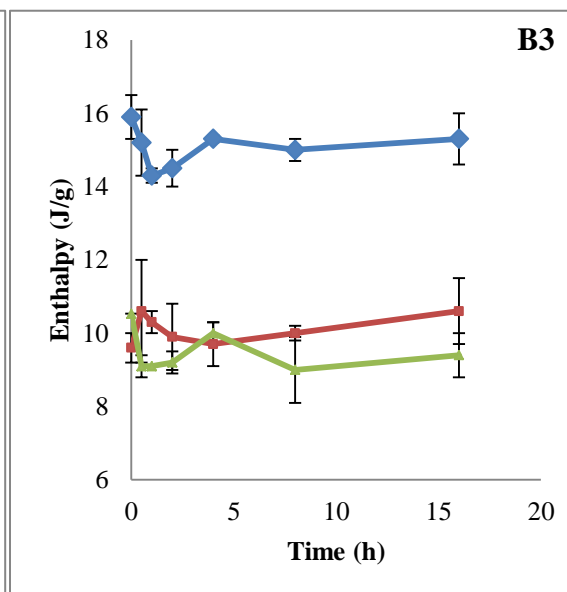
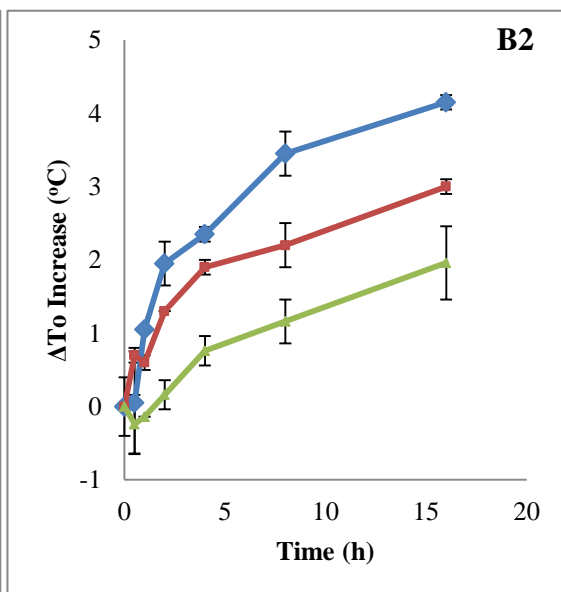
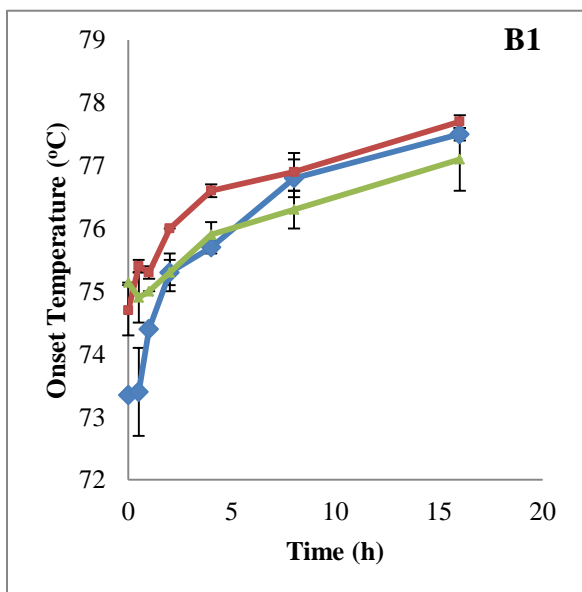
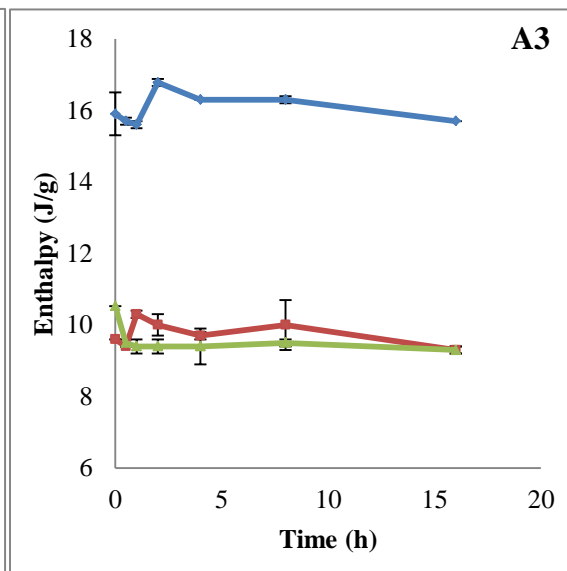
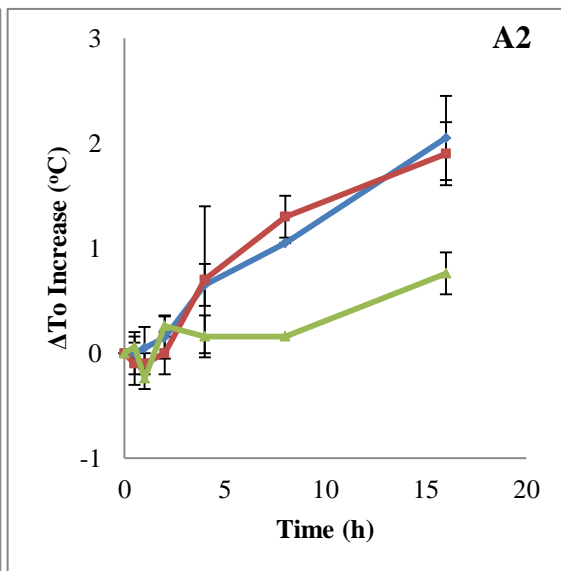
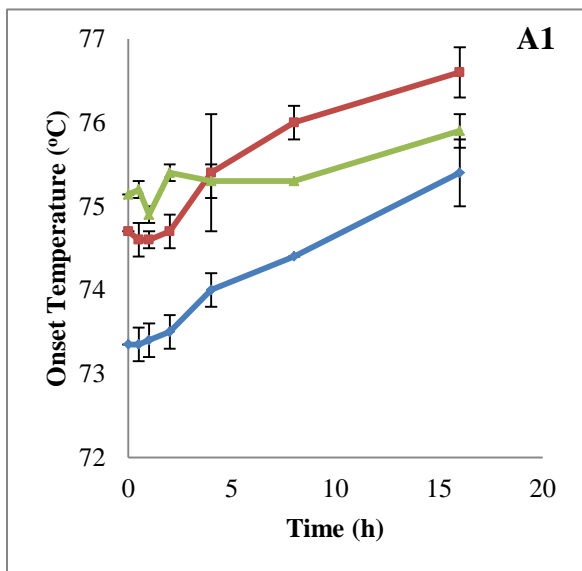


Figure 1-1 Water absorption of steeped (annealed) paddy, milled rice kernels and isolated starch steeped at 60°C (A) and 70°C (B).



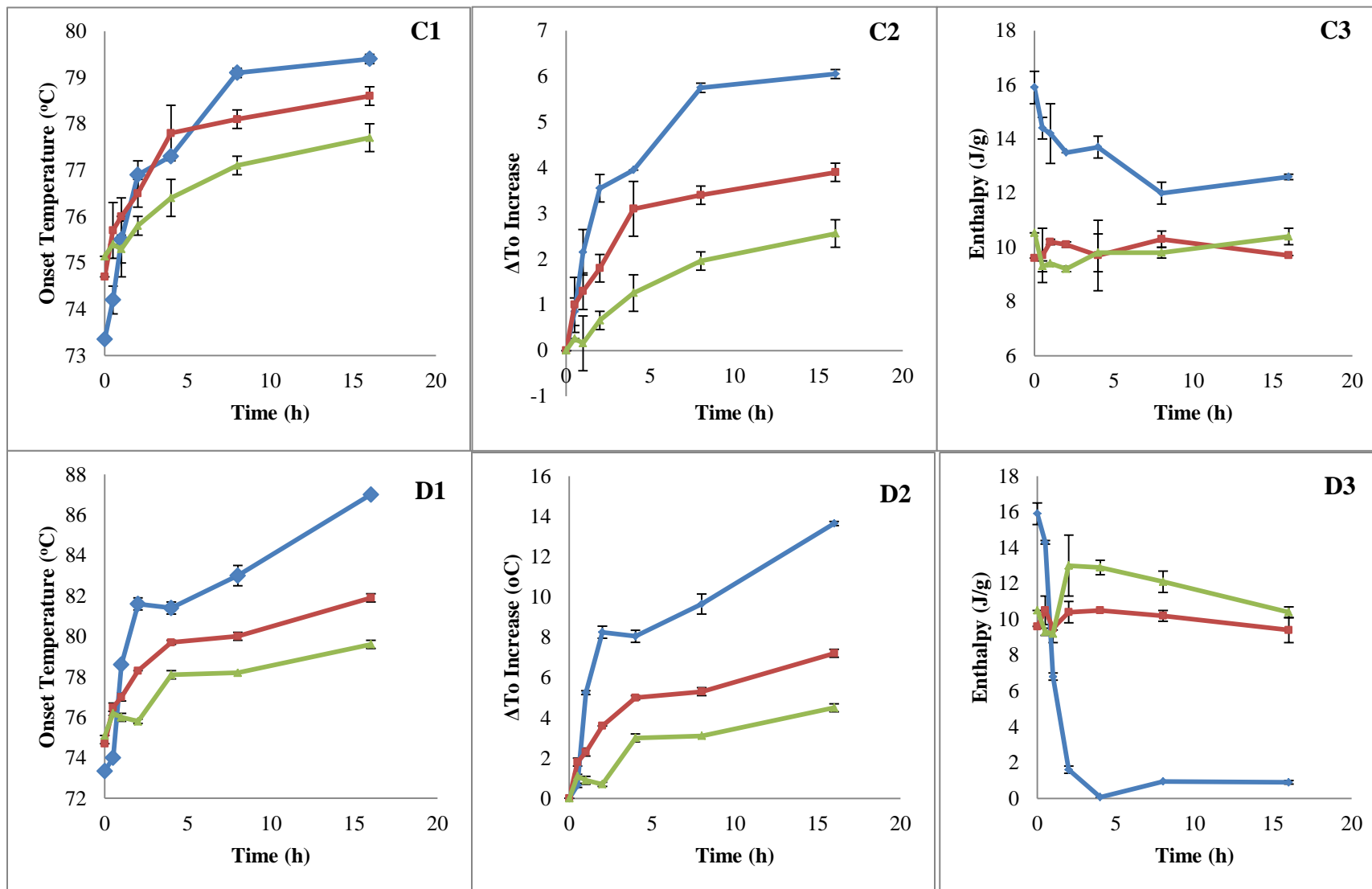


Figure 1-2 Onset gelatinization temperature (1), increase in T_0 (2), and enthalpy (3) of rice samples annealed at 60°C (A), 65°C (B), 70°C (C), and 75°C (D) up to 16h. (-◆- isolated starch, -■- milled rice, -▲- paddy rice)

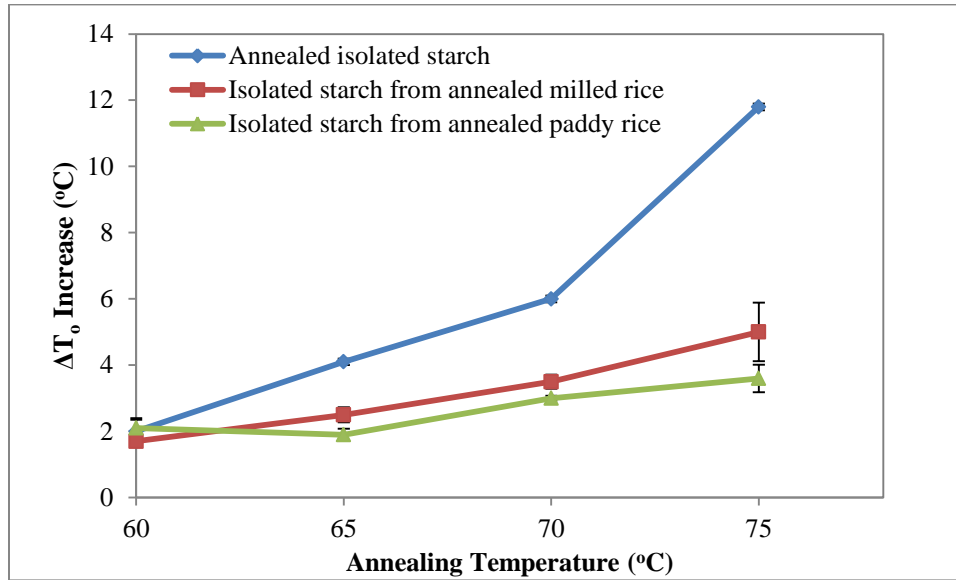


Figure 1-3 Increase in onset gelatinization temperature (ΔT_0) of 16h annealed starches from different rice sources and annealing temperatures. (-◆- isolated starch, -■- isolated starch from milled flour, -▲- isolated starch from paddy flour)

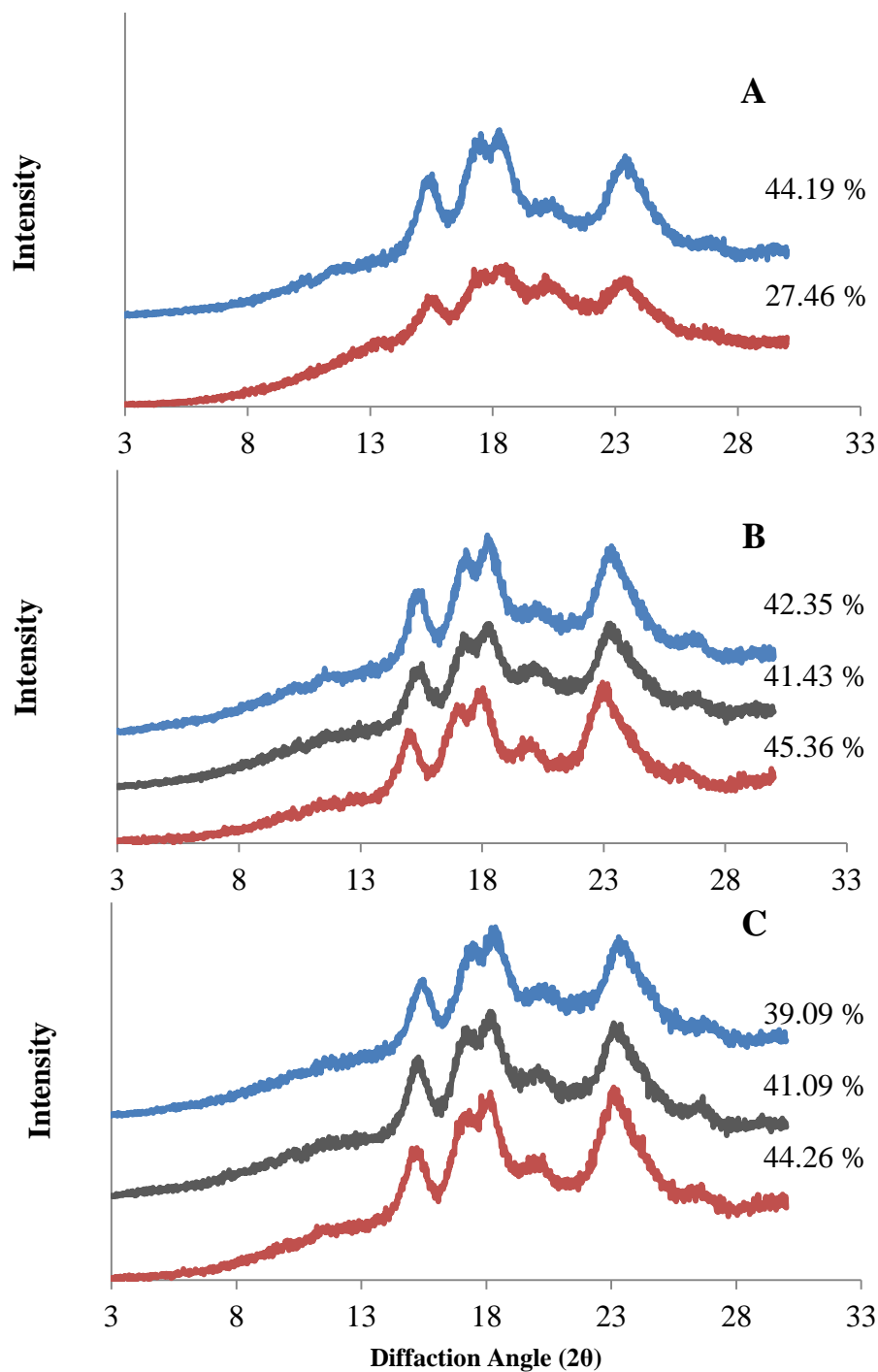
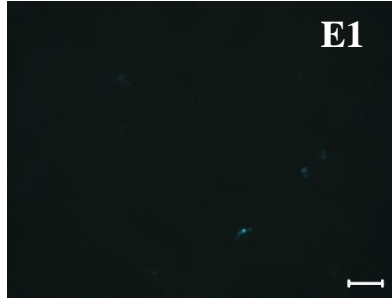
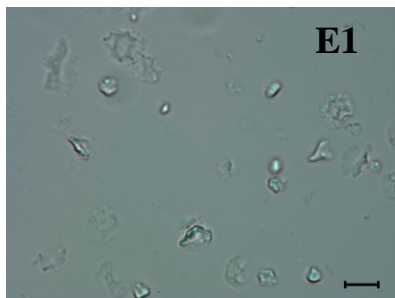
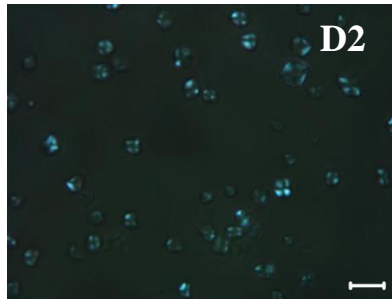
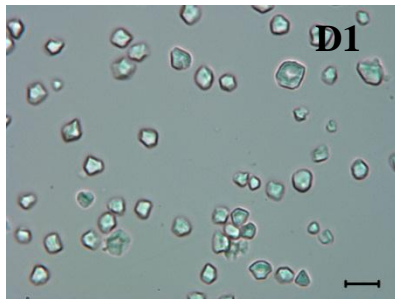
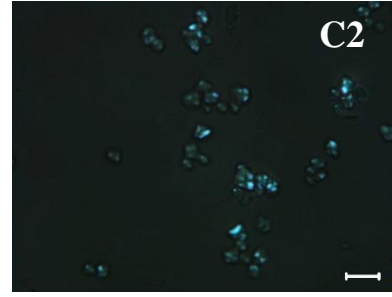
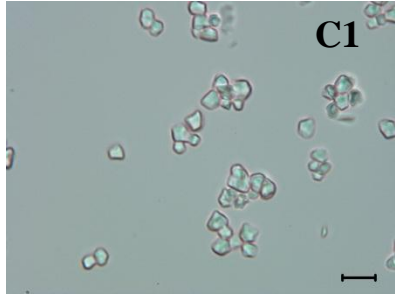
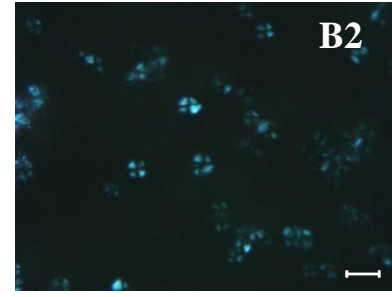
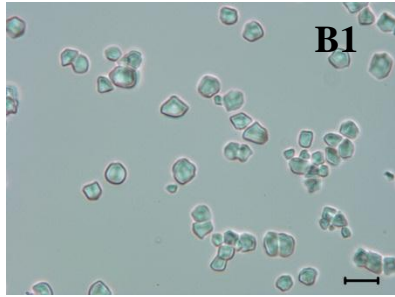
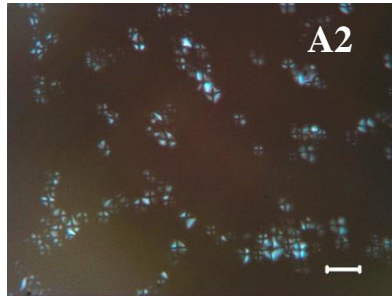
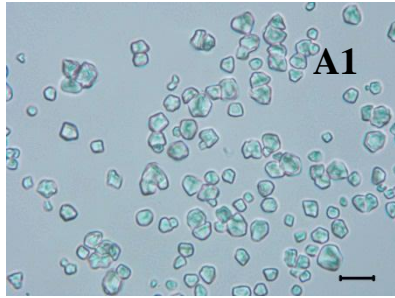


Figure 1-4 X-ray diffractograms of samples annealed at 75° for 16h. Isolated starch and annealed isolated starch (A), native milled flour, annealed milled flour, and isolated starch from annealed milled flour (B), native paddy flour, annealed paddy flour, and isolated starch from annealed paddy flour (C) (top to bottom curve, respectively). The values next to curve are degree of crystallinity.



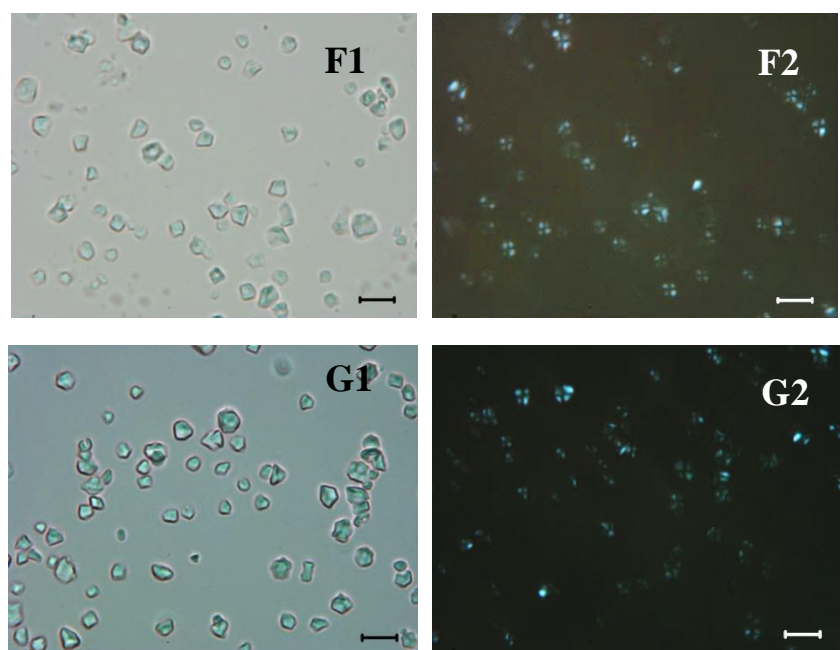
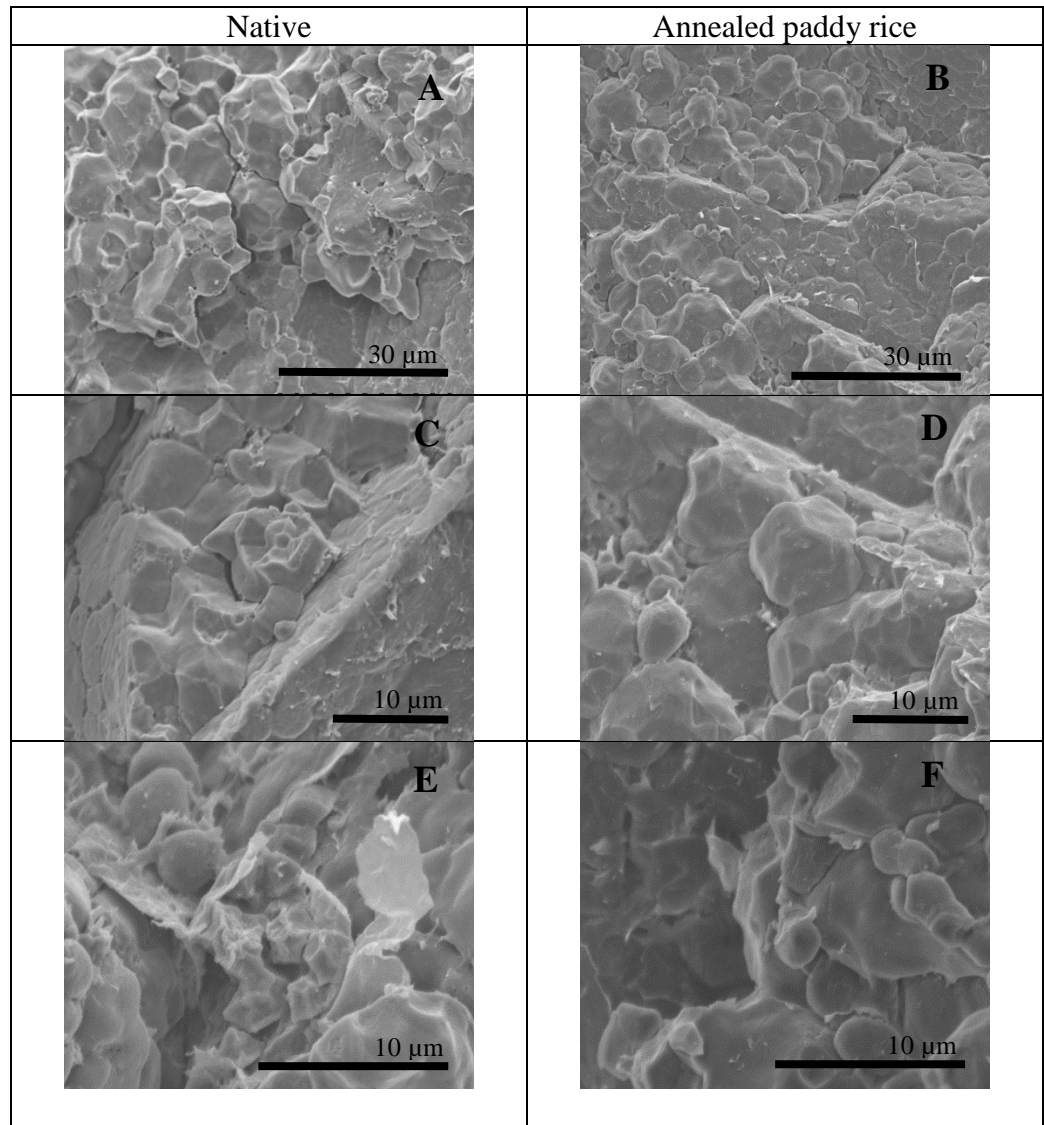


Figure 1-5 Photomicrographs of 16h annealed starches: native (A), 60°C (B), 65°C (C),70°C (D), 75°C (E) and starch isolated from annealed milled kernel at 75°C (F) and annealed paddy kernel at 75°C (F) at viewed under bright field (1) and polarized light (2) . (Scale bar = 10 μ m)



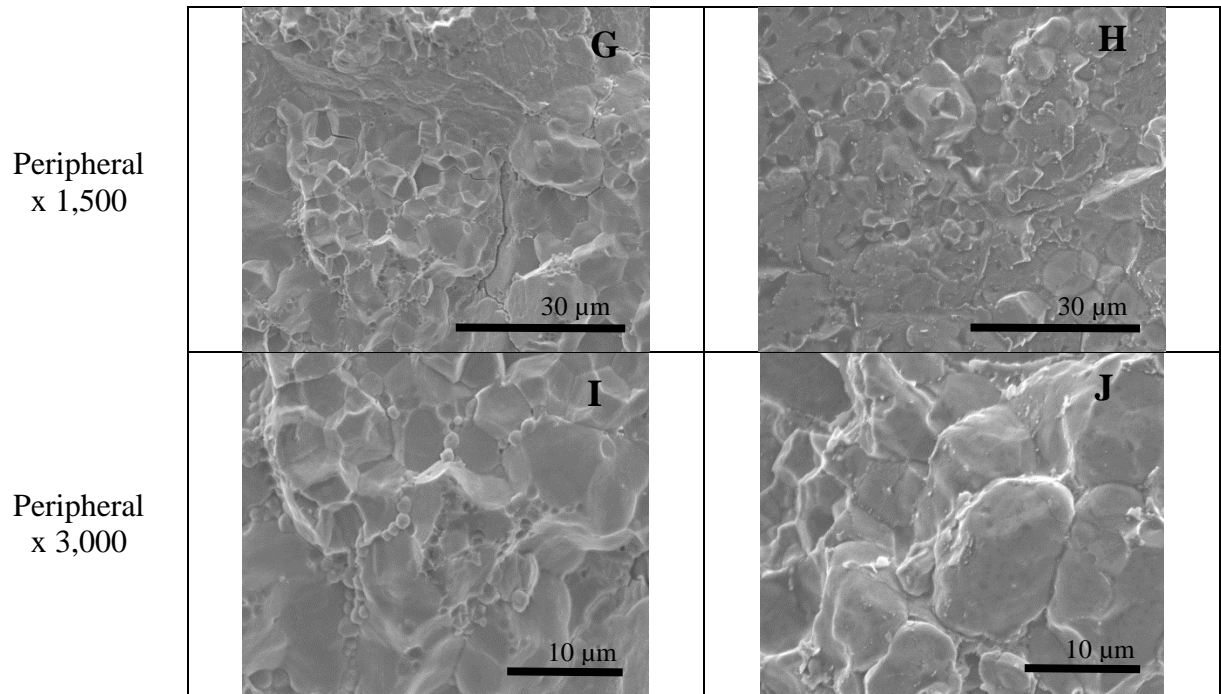
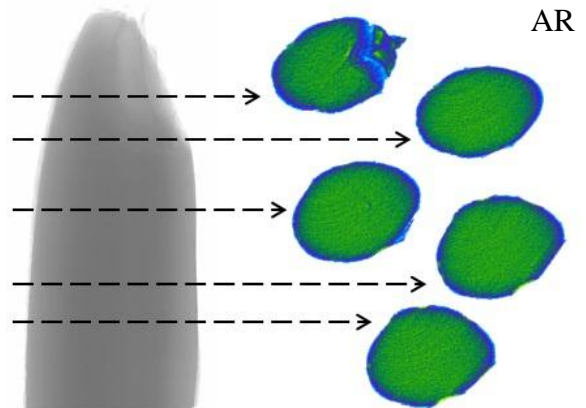
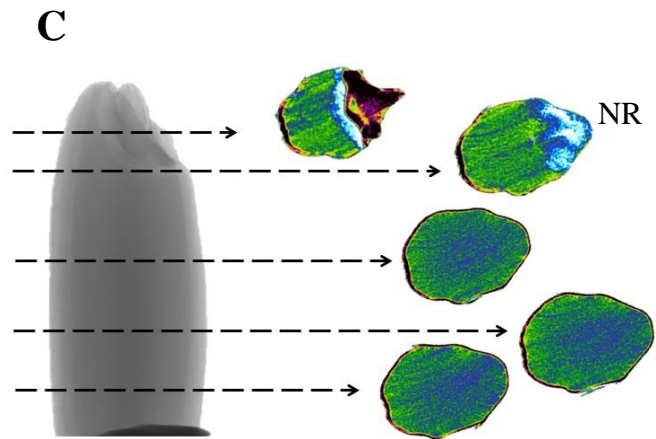
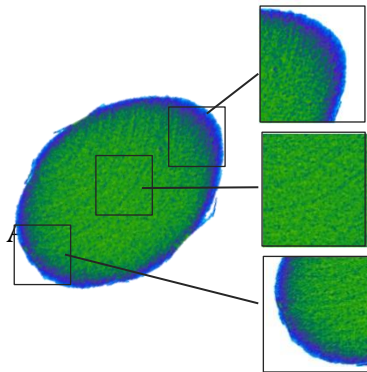
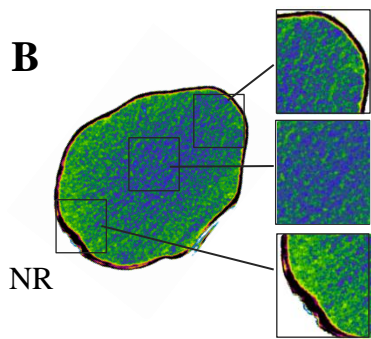
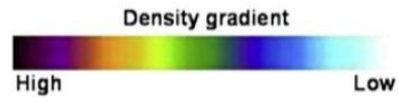
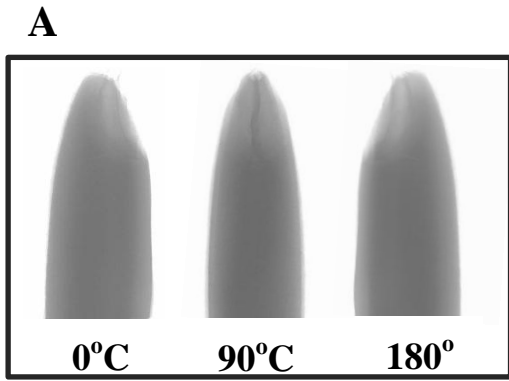


Figure 1-6 SEM cross-sections of native and 70°C 4h annealed paddy rice kernels at the interior (A-F) and peripheral regions (G-J) and at different magnifications.



D

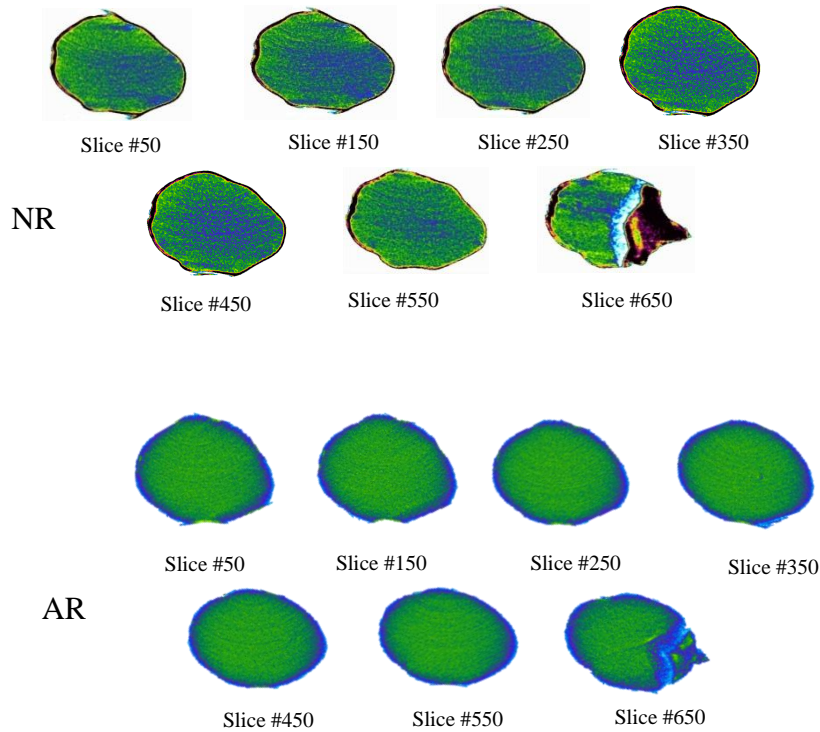


Figure 1-7 Rice kernel morphology was measured by X-ray microtomograph. NR= Native rice kernel, AR= Rice kernel annealed at 70°C for 16h. X-ray shadow (raw) images of rice kernels taken at different incremental angles (A). Expanded images for different parts of a rice 2-D sliced image (B). Density distribution of within kernels (C). 2-D crosssections images from different parts of kernels (D). The slice number reflects the position of the kernel. The higher the number, the closer to the tip of the kernel.

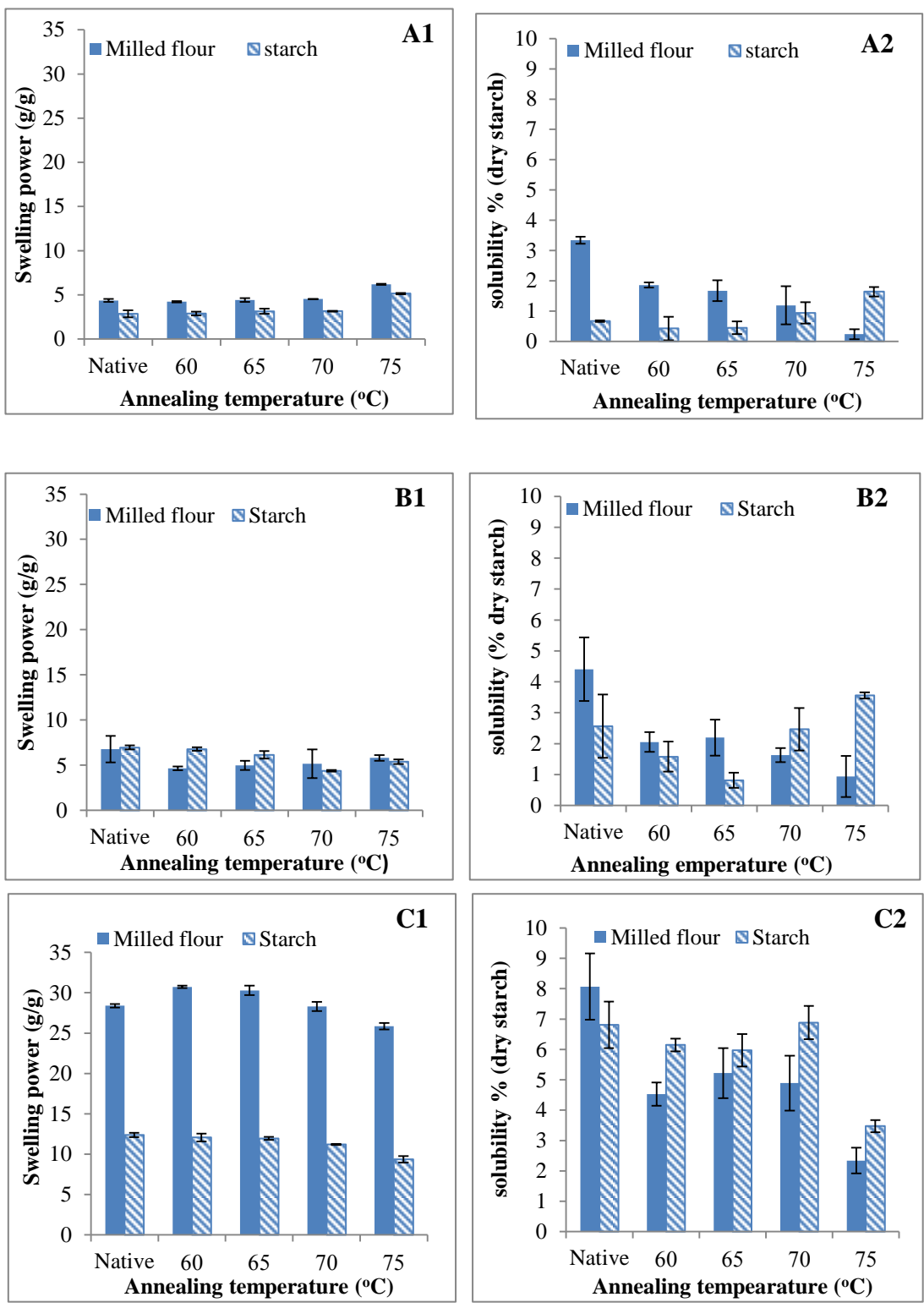


Figure 1-8 Swelling power (1) and solubility (2) of native and annealed starches and milled flour tested at 60°C (A), 75°C (B), and 90°C (C).

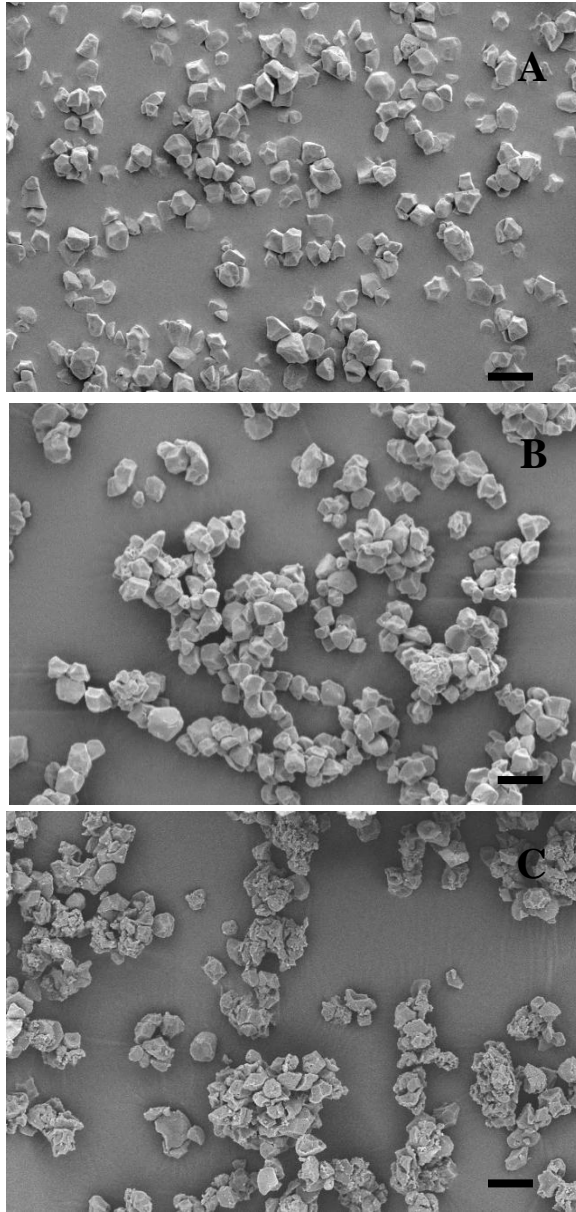


Figure 1-9 SEM of native rice starch (A), rice starch annealed at 70°C for 16h (B), and rice starch annealed at 75°C for 16h (C).
(Scale bar = 10 μm)

Chapter 2 - Changes in morphology of starch in parboiled rice kernels

Abstract

The morphologies of rice kernels and starch granules within rice kernels were examined immediately after the steaming process (110°C for 20 min) of parboiling. Fresh parboiled rice, parboiled rice aged one month, and commercial parboiled rice were studied to better understand the parboiling process. Starch was completely gelatinized as determined by DSC and XRD, indicating the disruption of all short-range crystallinity of starch in parboiled rice. However, SEM images showed intact starch granules, and light microscopic images showed starch granules embedded in the rice kernel. Interestingly, these granules displayed Maltese cross patterns. For the first time, we demonstrated that starch granules were birefringent and showed the Maltese cross but were not crystalline.

Introduction

Almost 20% of world rice production is made into parboiled rice (Buggenhout, Brijs, & Delcour, 2013). The parboiling process includes steeping, heating, and drying and greatly alters the characteristics of rice structure and cooking behavior (Priestley, 1976). Starch is gelatinized during the parboiling process, amylose and lipid complexes are formed (Derycke et al., 2005), and disulfide bonds are induced between proteins (Derycke et al., 2005). The extent of modification depends on processing conditions such as soaking time and temperature (Miah, Haque, Douglass, & Clarke, 2002), steaming time and temperature, moisture content (Derycke et al., 2005; Islam, Roy, Shimizu, & Kimura, 2002; Lamberts et al., 2006; Lamberts, Gomand, Derycke, & Delcour, 2009; Patindol, Newton, & Wang, 2008), and drying conditions. Soaking paddy rice to attain about 30% moisture content has been assumed to be sufficient to obtain complete gelatinization, but this is true only if water distribution is even within the grain (Bhattacharya, 2004). Uniform distribution of water is difficult, however, because the route, pattern, and speed of water penetration through a rice kernel can vary greatly depending on morphological structure, such as the packing of starch granules in the endosperm of each variety (Horigane, Takahashi, Maruyama, Ohtsubo, & Yoshida, 2006) and the degree of milling (Marshall, 1992). As a result, the amount of water in each region within the kernel certainly affects starch phase transition and physical properties. Ong and Blanshard (1995) suggested three major polymorphic forms of starch crystallinity in parboiled rice that may explain its unique cooking behavior: residual starch, which consists of starch of low melting temperature and high melting temperature as a result of prolonged steeping under favorable conditions; retrograded starch; and amylose-lipid complexes. Derycke and Delcour (2005) studied how proteins affect the cooking properties of parboiled rice. The proteins in rice endosperm act as barriers to water

penetration in both native and parboiled rice. These proteins restrict starch granules' swelling during thermal processes and appear to be strengthened (made denser) by reduced protein extractability after parboiling (Buggenhout et al., 2013). Lipid and amylose are also known to restrict swelling and solubilization of starch during cooking (Tester & Morrison, 1990).

Under proper conditions, parboiled paddy rice kernels expand but are restricted within the void space inside the hull. It is not well documented how parboiling affects starch granule morphology, as they are embedded in the rice grain. In this study, we emphasized a histological view of parboiled rice kernels. We carefully examined parboiled rice starch granules immediately after the steaming process by light microscopy, scanning electron microscopy (SEM), differential scanning calorimetry (DSC), and X-ray diffraction (XRD), to gain a better understanding of the morphological and phase transition of starch within parboiled rice kernels.

Materials and methods

Materials

Long-grain paddy rice was obtained from Mars Food US, Llc. (Los Angeles, CA). Foreign matter was removed by sifting through 10-mesh and 16-mesh standard test sieves (Fisher Scientific, Pittsburg, PA) and dehulled with a McGill Sheller (McGill Inc., Houston, TX). Chemicals were analytical grade.

Parboiling of rice

Parboiling treatment was achieved using a laboratory autoclave. Pre-soaked (70°C for 4h) paddy rice kernels were placed on perforated trays inside the autoclave chamber to allow even heat distribution and excess water to drain. The temperature was ramped up to 110°C and held at

this temperature for 20 min. Pressure was maintained at 0.7 bar throughout the experiment. After 20 min, the pressure was released and samples were removed. Each grain was individually dehulled by hand. Dehulled kernels were gently ground by a mortar and pestle.

Kernel size determination

Immediately after steaming, hulls were manually removed from fresh parboiled rice. Kernel length and width were measured using a digital caliper (Model CD-S8”M, Mitutoyo, Japan). The same was done for dehulled native kernels. Twenty kernels were measured per sample.

Light microscopy

Immediately after steaming, hulls were manually removed and each kernel was split in half. Endosperm content was gently removed from the kernel and placed on a glass slide and two drop of an iodine and potassium iodide solution (0.313 g of iodine and 7.5 g of potassium iodide in 500 mL of 50% glycerol) were added and held for 10 min in the dark before viewing.

Microtome slices were prepared according to the procedure found in **Appendix D**.

Differential scanning calorimeter

Thermal properties were determined in duplicate by a DSC (DSC Q100, TA Instruments, New Castle, DE). Approximately 9 mg of starch was accurately weighed into a high volume stainless steel sample pan. Distilled water was added to obtain a starch to water ratio of 1:2 (w/w). The sample pans were hermetically sealed and heated from 10°C to 120°C at the rate of 10°C/min. Reported transition temperatures were gelatinization onset (T_o), peak (T_p), and conclusion (T_c). The enthalpy of gelatinization (ΔH) was calculated using Universal Analysis (TA Instruments) and normalized to dry weight of sample.

X-ray diffraction

X-ray diffraction was conducted with a X-ray diffractometer (APD 3520, Philips, Eindhoven, Netherlands) with Cu K α radiation at 35 kV and 20 mA, a theta-compensating slit, and a diffracted beam monochromator. The diffractograms were recorded from 3° to 30° (2 θ). Relative crystallinity was estimated by the ratio of the peak areas to the total diffractogram area. [Detailed calculation methods can be found in **Appendix C.**]

Scanning electron microscopy

Rice kernel morphology was examined by SEM (S-3500N, Hitachi Science Systems, Ltd., Japan) at an accelerating potential of 5 kV using X-ray Detector-Link Pentafet 7021 (Oxford Instruments Microanalysis Limited, Bucks, England). Each grain was manually fractured at the middle, and a blade was used to trim off the bottom end. The fractured cross-sections of the kernel were mounted face up on an aluminum stud using double-sided adhesive tape and sputter-coated with gold palladium (60:40 ratio) 3 times for 20 s under vacuum with a Desk II Sputter/Etch Unit (Denton Vacuum, LLC, Moorestown, NJ) before viewing.

Statistical analysis

Data were analyzed by analysis of variance (ANOVA) with the Duncan multiple range test using SAS version 9.1 (SAS Institute, Inc., Cary, NC, USA). Mean values and standard deviation of replications were reported.

Results and discussion

Thermal and crystalline properties of fresh parboiled rice

Unlike native rice flour, freshly parboiled rice displayed no endotherm peak (Fig.1D) for the melting of crystallites from amylopectin ($\sim 70^{\circ}\text{C}$) or amylose-lipid complex ($>100^{\circ}\text{C}$) (Fig. 2.1A). Heat treatment at 110°C for 20 min at 35% initial moisture content appears to be sufficient to destroy all short-range crystalline order, as detected with DSC. The sample aged at 25°C for one month was scanned, and two separate endotherms were observed (Fig. 2.1C). The first endotherm at 60°C is the result of the melting of reassociated (retrograded) amylopectin. The second endotherm at 110°C is in the range of the melting of amylose-lipid complex (Biliaderis & Galloway, 1989). Our data suggest that the majority of starch molecules are in non-associated form immediately after heat treatment. Reassociation occurred only upon ageing (drying), and was revealed by DSC.

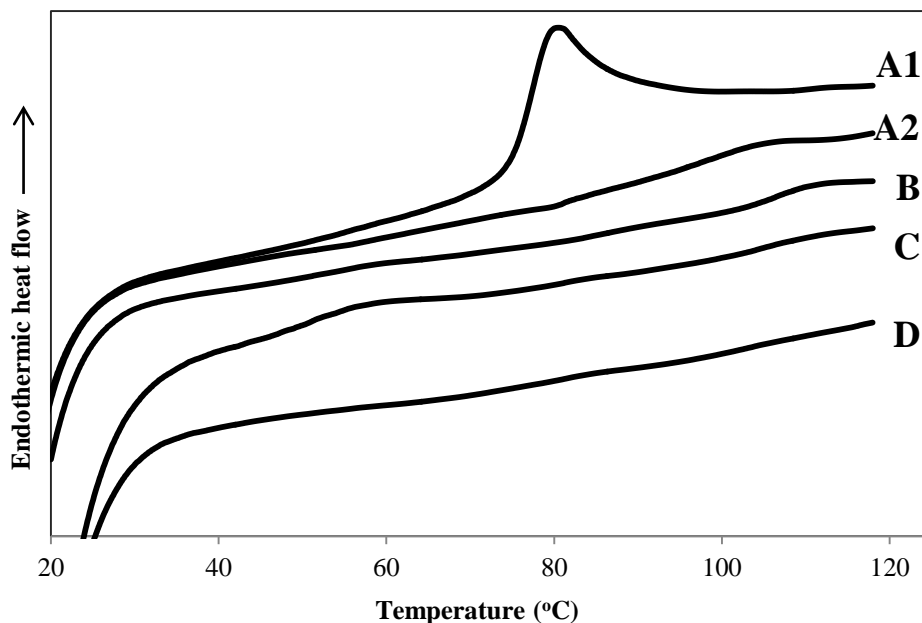


Figure 2-1 DSC thermogram of native rice flour- first scan (A1); native rice flour- second scan (A2); commercial parboiled rice (B); aged parboiled rice flour (C); and fresh parboiled rice flour (D).

The XRD diffractogram presents crystallinity polymorphism of starch after parboiling and after storage at room temperature for one month (Fig. 2.2). Native rice flour displayed a typical A-type pattern with peaks at $2\theta = 15^\circ, 17^\circ, 18^\circ$ and 23° . Freshly parboiled rice was completely amorphous; no A-type patterns from residual amylopectin were seen, which was in agreement with DSC thermogram. Although a slight peak at $2\theta = 20^\circ$ suggests a V_h -type pattern from the formation of amylose-lipid complexes during parboiling, which was also detected by DSC (Fig. 2.1A2). Aged parboiled rice had high intensities at $2\theta = 13^\circ, 20^\circ$ (V_h -type crystallites) which is in agreement with the DSC 2nd endothermic peak of amylose-lipid complex. A weak A-type pattern was also seen at $2\theta = 15^\circ, 17^\circ, 18^\circ$, and 23° ; however, an endothermic peak around 75°C was not detected by DSC. Therefore, the A-type crystallites observed in our XRD results must not be from residual starch, as previously suggested by Derycke et al. (2005), but are more

likely from retrograded amylopectin. B-type XRD patterns in our aged rice were not detected, which suggests that A-type crystallites were formed during drying and ageing. In studying enzyme resistant starches, Eerlingen et al. (1993) also reported that retrograded gelatinized wheat starch can result in A- or B-type crystallinity depending on (re)crystallization temperature and speed. Cai and Shi (2013) noted that formation of A- and B-type spherulites from short-chain debranched amylose can be formed, depending on crystallization conditions. Higher temperatures (50°C) during crystallization result in A-type crystals, whereas B-type crystals are formed at lower temperatures (25°C). The XRD pattern of a commercial parboiled rice is similar to aged parboiled rice, except that intensity is stronger $2\theta = 20^{\circ}$ and very low around $2\theta = 17-18^{\circ}$. This result suggests that the commercial parboiled rice was processed at a higher temperature or a combination of temperature and pressure that induced more amylose-lipid formation and limited retrogradation during processing and storage. It should also be noted that the rice variety used for the commercial parboiled rice may be different than the rice used in this study.

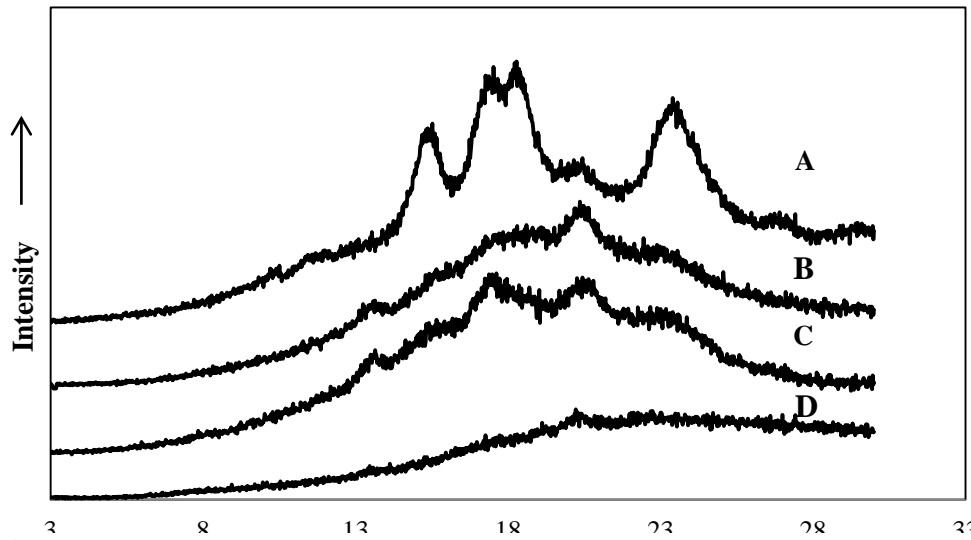


Figure 2-2 XRD diffractogram of native starch (A), commercial parboiled rice flour (B), aged parboiled rice flour (C), and fresh parboiled rice flour (D).

Morphological structure of parboiled rice

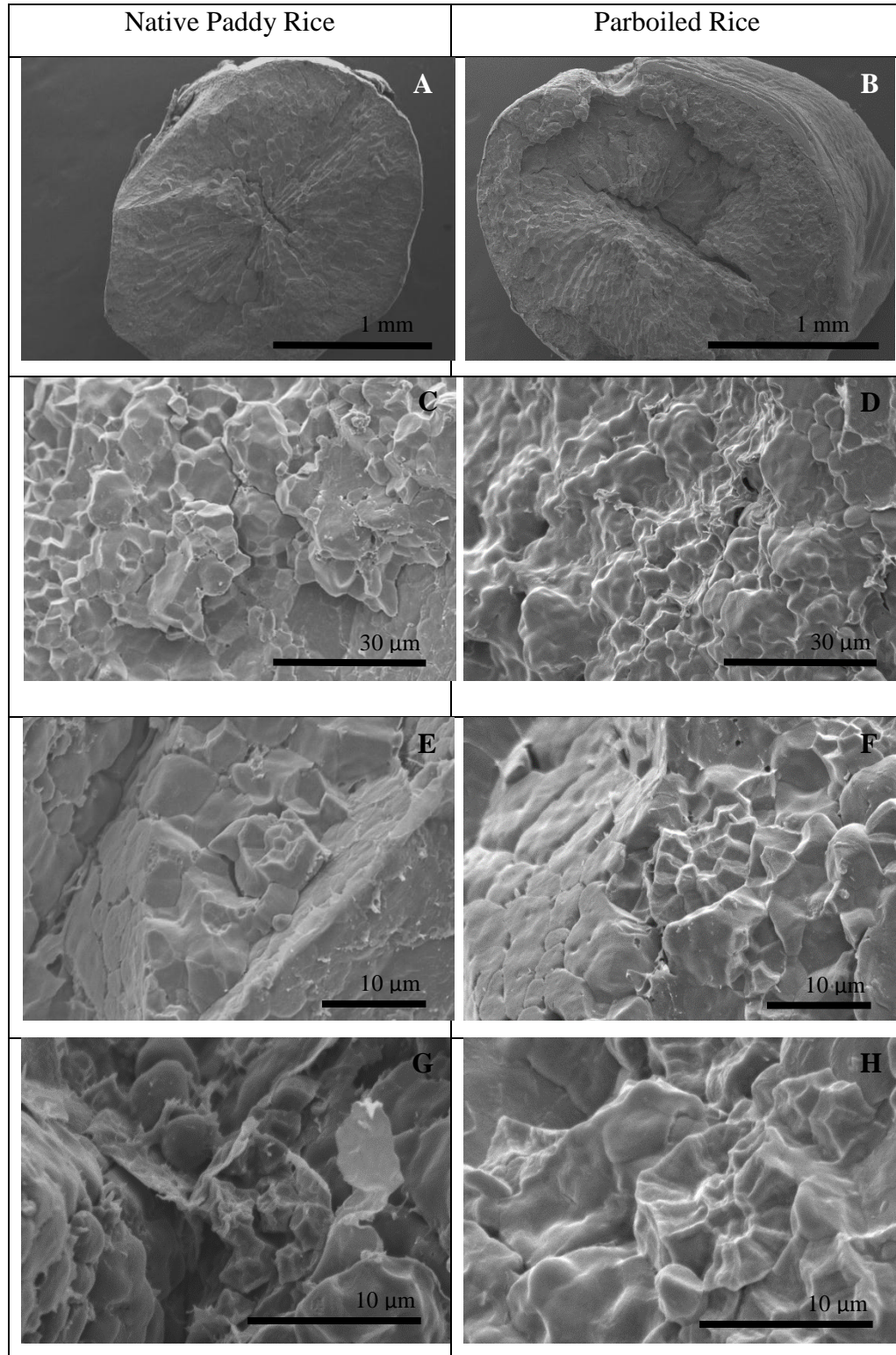
Soaking paddy rice, originally 12% moisture content, at 70°C for 4 h increased moisture content 36%. Interestingly, the kernels had similar moisture content before and after parboiling at 110°C for 20 min although kernel size appeared larger. Immediately after parboiling, rice kernels were significantly bigger (Table 2.1). Length and width of fresh parboiled kernels increased by 4.21 and 10.37%, respectively, compared with the native kernels.

Table 2-1 Kernel moisture content and size

Sample	Native brown rice kernel	Parboiled rice kernel (fresh, dehulled)
Moisture content (%)*	12.01± 0.37 b	35.15 ±0.33 a
Length (mm)**	6.54±0.27 b	6.82 ± 0.37 a
Width (mm)**	2.10±0.092 a	2.35 ± 0.095 b

^a Values in the same row followed by the same letter are not significantly different ($P < 0.05$)

Fig. 2.3 shows SEM cross-section of native brown rice and parboiled rice. At the center of the kernel surface in native rice, compound granules were observed and some were broken, exposing individual polygonal rice granules (Figs. 2.3C-H). Some individual granules remained visible in parboiled kernels but appeared slightly fused, and lost their polygonal shape. Under high magnification, native rice starch granules are clearly polygonal shapes around 3 μm and fit together tightly in a compound granule (Fig. 2.3G). Fresh parboiled granules are about 5 μm (Fig. 2.3H) and appear merged together, although individual granule shapes can still be observed. The peripheral outer layer, on the other hand, has small protein bodies scattered throughout the surface, mainly embedded in cracks between granules. Parboiled kernels have proteins that appear aggregated together.



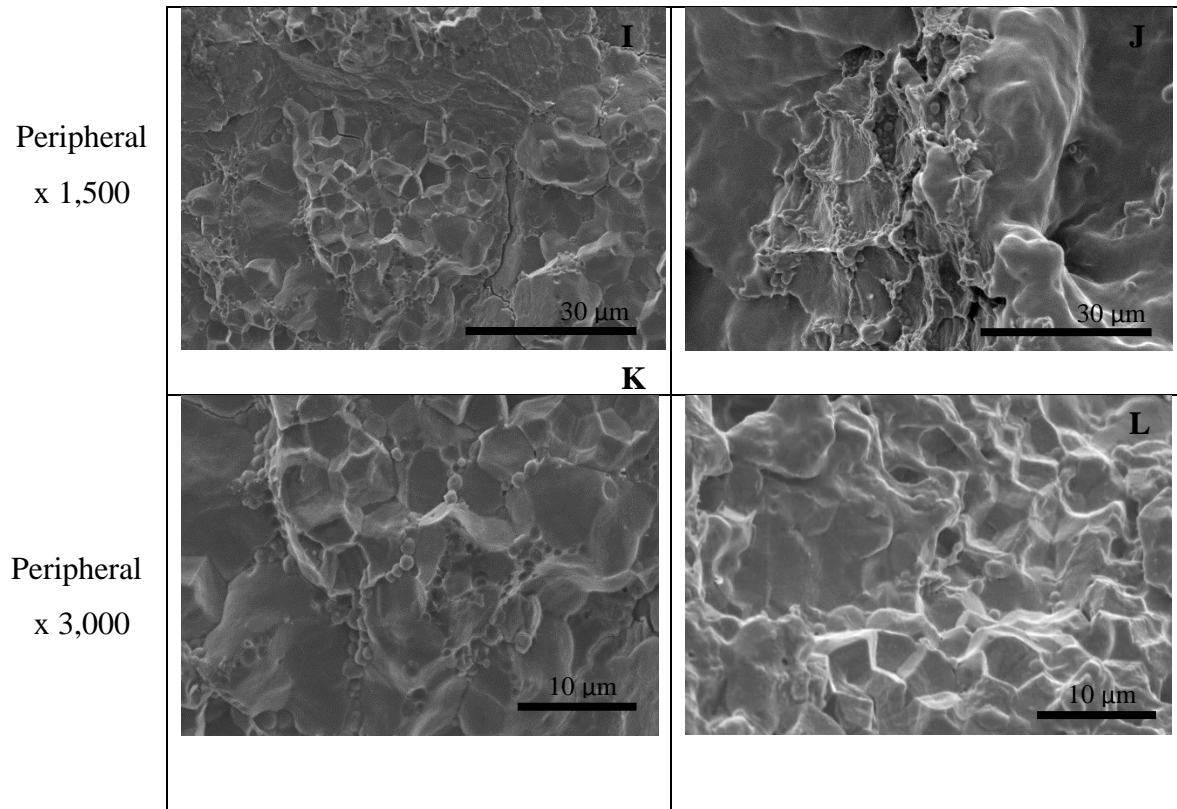


Figure 2-3 SEM cross-sections of native and parboiled rice kernels at the interior (A-H) and peripheral (I-L) regions at different magnifications.

Microscopic investigation of freshly parboiled rice endosperm in glycerol revealed that the majority of samples did not display birefringence or a Maltese Cross. A few intact granules were found in parboiled rice (Fig. 2.5A-C). Starch granules embedded in a large flour particle remained birefringent (Fig. 2.5D). Those granules were around 20 μm , almost 4 times the size of native rice granules (Fig. 2.4). Assuming that the average particle size of native rice starch is 5 μm (in solution), the granules swelled dramatically. Yet, these granules revealed Maltese cross under polarized light. It has been noted that in the absence of shear, starch granules can swell to many times their original size while maintaining their integrity (Parker & Ring, 2001), however, a Maltese cross pattern was not reported. Also, since samples were observed immediately after parboiling, our data could not be the result of the regaining of birefringence as observed by

Jacobson, Obanni & Bemiller (1997). In addition, these authors did not observe the regaining of Maltese Cross patterns.

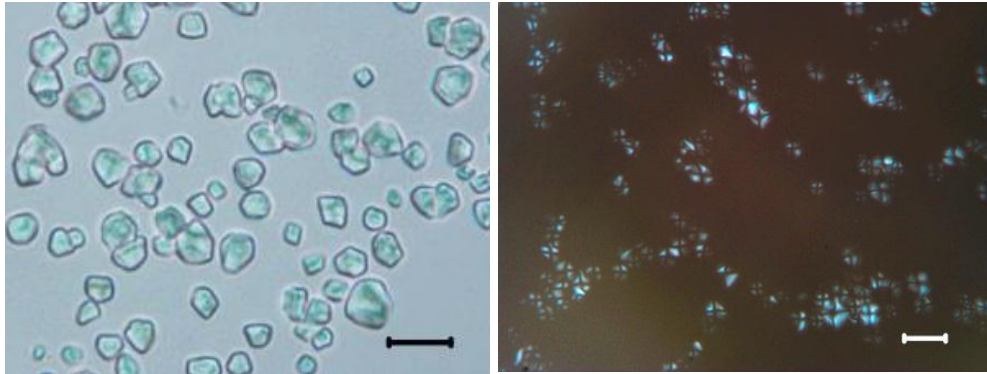


Figure 2-4 Photomicrograph of native rice starch under bright field and polarized light at x100 oil immersion lens. (Scale bar = 10 μm)

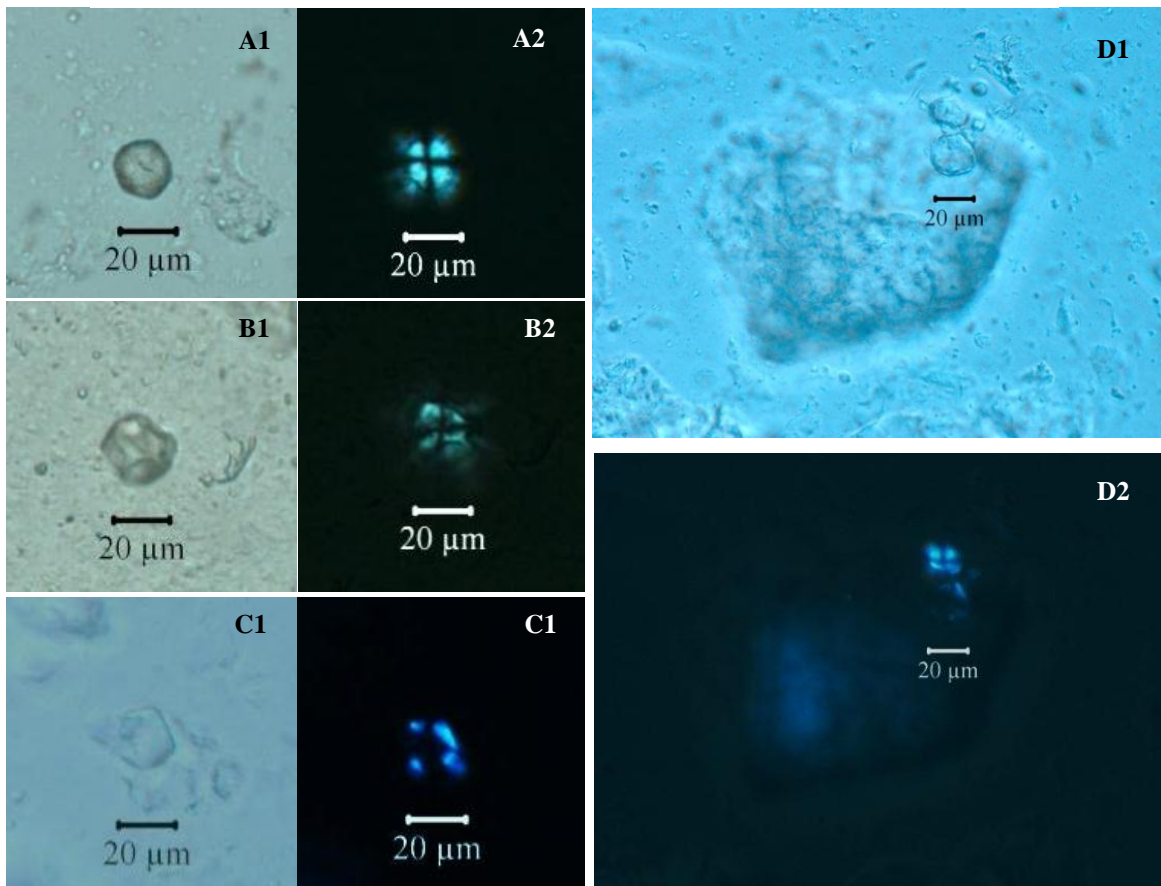


Figure 2-5. Photomicrographs of fresh parboiled rice flour (A-D) under (1) bright field and (2) polarized light at 40x objective. (Scale bar = 10 μm)

Microscopic photomicrographs also reveal that starchy endosperm cells (thin-walled parenchyma cells) of interior regions appear intact, whereas peripheral regions were disrupted due to gelatinization (Fig. 2.6). Our results are in agreement with Ogawa et al. (2003), who studied the morphological structure of microwaved cooked rice kernels and suggested that structures in cooked grain are heterogeneity. The authors found that the cell walls of peripheral cells were more disrupted than the center region where accessibility of moisture is limited and results in a lower degree of modification. A polarized view (Fig. 2.7) of the parboiled rice cross-section also reveals very small, but visible Maltese cross patterns. These granules are less than 5 μm .

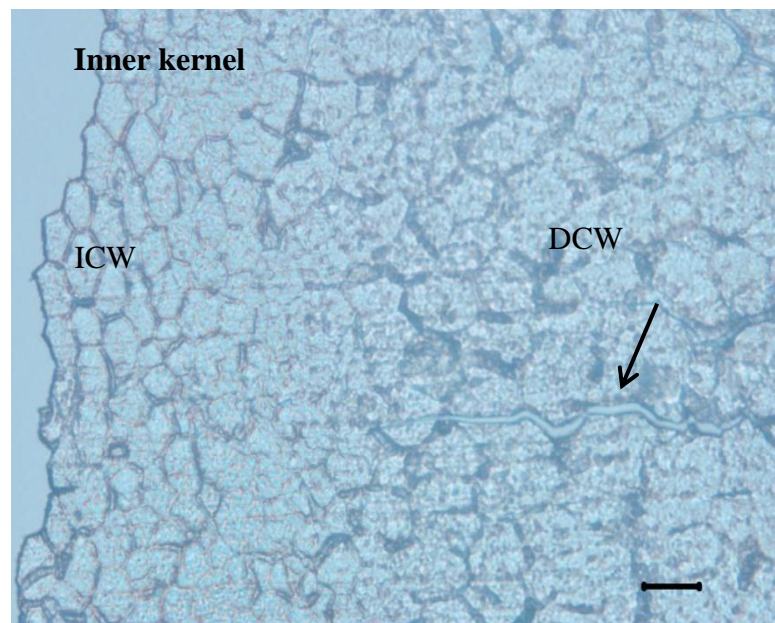


Figure 2-6 Microtome longitudinal section of parboiled rice kernel viewed under bright field microscope. Note intact cell wall (ICW), disrupted cell wall (DCW) and crack in the starchy endosperm as indicated with arrow. (Scale bar = 20 μm)

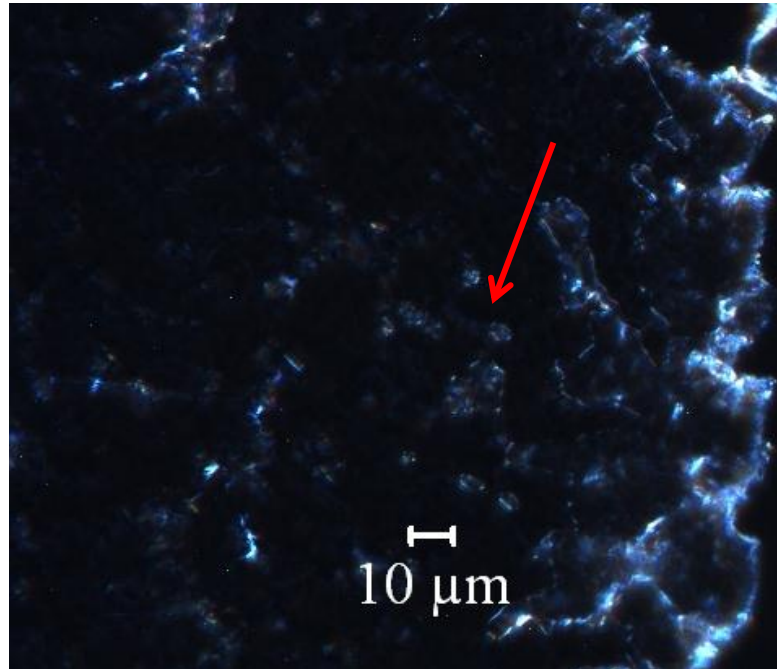


Figure 2-7 Microtome longitudinal section of parboiled rice kernel viewed under dark field microscope. Arrow indicates area with Maltese Cross.

With limited moisture (~36% water) and restricted space during parboiling, our data revealed that starch was completely gelatinized as determined by DSC and XRD, indicating the disruption of all short-range crystallinity of starch in the parboiled rice. The Maltese Cross is the complementary dark pattern dividing four bright quadrants which is the result of radially oriented molecules in the starch granule as their optic axes pass through two polarized filter (Evans, McNish, & Thompson, 2003). Symmetrically and radially oriented starch chains are perpendicular to the starch surface. Therefore, our data suggests that this level of orientation maintains though parboiling. We determined that starch was uniquely transformed during

parboiling; and although short-range crystallinity was destroyed, its long-range order was retained.

Conclusions

In this study, parboiled rice was completely gelatinized as detected by immediate DSC and XRD analysis. After storage at room temperature, amorphous starch (re)associated to form a mixed A- type and V_h - type diffraction patterns from retrograded starch and amylose-lipid complexion respectively. Histological properties of fresh parboiled rice kernels revealed a “fused” mass that maintained the appearance of individual starch granules, especially in the interior region of the kernel. Rice protein aggregation was observed in the peripheral region. Interestingly, some intact granules displayed Maltese cross patterns, demonstrating that parboiling is a unique process that results in starch granules that are not crystalline but nevertheless display Maltese cross.

Reference

- Bhattacharya, K. R. (2004). Rice: Chemistry and technology. In E. T. Champagne (Ed.), (3rd ed., pp. 329-404). St. Paul, Minn.: American Association of Cereal Chemists.
- Biliaderis, C. G., & Galloway, G. (1989). Crystallization behavior of amylose-V complexes: Structure-property relationships. *Carbohydrate Research*, 189, 31-48.
- Buggenhout, J., Brijs, K., & Delcour, J. A. (2013). Impact of processing conditions on the extractability and molecular weight distribution of proteins in brown parboiled rice. *Journal of Cereal Science*, 58(1), 8-14.
- Evans, A., McNish, N., & Thompson, D. B. (2003). Polarization colors of lightly Iodine-stained maize starches for Amylose-Extender and related genotypes in the W64A inbred line. *Starch-Stärke*, 55(6), 250-257.
- Cai, L., & Shi, Y.-C. (2013). Self-assembly of short linear chains to A-and B-type starch spherulites and their enzymatic digestibility. *Journal of Agricultural and Food Chemistry*, 61(45), 10787-10797.
- Derycke, V., Vandeputte, G., Vermeylen, R., De Man, W., Goderis, B., Koch, M., & Delcour, J. (2005). Starch gelatinization and amylose–lipid interactions during rice parboiling investigated by temperature resolved wide angle X-ray scattering and differential scanning calorimetry. *Journal of Cereal Science*, 42(3), 334-343.
- Derycke, V., Veraverbeke, W., Vandeputte, G., De Man, W., Hosoney, R., & Delcour, J. (2005). Impact of proteins on pasting and cooking properties of nonparboiled and parboiled rice. *Cereal Chemistry*, 82(4), 468-474.
- Eerlingen, R. C., Crombez, M., & Delcour, J. A. (1993). Enzyme-resistant starch. I. quantitative and qualitative influence of incubation time and temperature of autoclaved starch on resistant starch formation. *Cereal Chemistry*, 70(3), 339-344.
- Horigane, A. K., Takahashi, H., Maruyama, S., Ohtsubo, K., & Yoshida, M. (2006). Water penetration into rice grains during soaking observed by gradient echo magnetic resonance imaging. *Journal of Cereal Science*, 44(3), 307-316.
- Islam, M. R., Roy, P., Shimizu, N., & Kimura, T. (2002). Effect of processing conditions on physical properties of parboiled rice. *Food Science and Technology Research*, 8(2), 106-112.
- Jacobson, M. R., Obanni, M., & Bemiller, J. N. (1997). Retrogradation of starches from different botanical sources 1. *Cereal Chemistry*, 74(5), 511-518.

- Lamberts, L., Bie, E. D., Derycke, V., Veraverbeke, W., De Man, W., & Delcour, J. (2006). Effect of processing conditions on color change of brown and milled parboiled rice. *Cereal Chemistry*, 83(1), 80-85.
- Lamberts, L., Gomand, S. V., Derycke, V., & Delcour, J. A. (2009). Presence of amylose crystallites in parboiled rice. *Journal of Agricultural and Food Chemistry*, 57(8), 3210-3216.
- Marshall, W. E. (1992). Effect of degree of milling of brown rice and particle size of milled rice on starch gelatinization. *Cereal Chemistry*, 69(6), 632-636.
- Miah, M., Haque, A., Douglass, M. P., & Clarke, B. (2002). Parboiling of rice. part II: Effect of hot soaking time on the degree of starch gelatinization. *International Journal of Food Science & Technology*, 37(5), 539-545.
- Ogawa, Y., Glenn, G. M., Orts, W. J., & Wood, D. F. (2003). Histological structures of cooked rice grain. *Journal of Agricultural and Food Chemistry*, 51(24), 7019-7023.
- Ong, M. H., & Blanshard, J. (1995). The significance of starch polymorphism in commercially produced parboiled rice. *Starch-Stärke*, 47(1), 7-13.
- Parker, R., & Ring, S. (2001). Aspects of the physical chemistry of starch. *Journal of Cereal Science*, 34(1), 1-17.
- Patindol, J., Newton, J., & Wang, Y. (2008). Functional properties as affected by Laboratory-Scale parboiling of rough rice and brown rice. *Journal of Food Science*, 73(8), E370-E377.
- Priestley, R. (1976). Studies on parboiled rice: Part 1—comparison of the characteristics of raw and parboiled rice. *Food Chemistry*, 1(1), 5-14.
- Tester, R. F., & Morrison, W. R. (1990). Swelling and gelatinization of cereal starches. I. effects of amylopectin, amylose, and lipids. *Cereal Chemistry*, 67(6), 551-557.
- Zobel, H. (1988). Molecules to granules: A comprehensive starch review. *Starch-Stärke*, 40(2), 44-50.

Appendix A

Detailed procedure for using oil immersion lens

Apparatus:

- a. Light microscope (Olympus BX51, Olympus America Inc., Melville, NY).
- b. SPOT Insight camera and SPOT ADVANCE software (Diagnostic Instruments Inc., Sterling Heights, MI)
- c. Plain microscope slides (Fisherbrand, Fisher Scientific International Inc.)
- d. Eppendorf
- e. 200 μ l Pippett

Reagents:

- a. Pure glycerol (Fisher Scientific International, Inc.)
- b. Immersion oil for microscopy, ordinary use (Olympus, Japan)

Sample preparation:

- a. Flour or starch finely ground
- b. Disperse approx. 10 mg of sample in \approx 2 ml in water solution in an 2 ml eppendorf tube

Microscope evaluation:

- a. Transfer a single drop of sample solution to a glass slide using a pipette and place the slide in position on the microscope under low magnification
- b. Adjust coarse and fine adjustment knob until image is clear
- c. Add a single drop of immersion oil slightly to the side of the sample droplet

- d. Slowly move the x100 immersion lens, into position. **Note:** Lens should pass the oil droplet before immersing directly in the sample.
- e. Adjust fine adjustment knob until image is clear
- f. Images were captured and analyzed through the SPOT Advance program

Appendix B

Detailed procedure for isolating rice starch

Apparatus:

- a. Grinder - (Waring blender 7011 Model 31BL92, New Hartford, CN)
- b. pH controller
- c. Water baths –large capacity with covers; capable of maintaining temperatures of.
- d. Oven- convection, set at 40°C
- e. Timer
- f. Pipettes
- g. Magnetic stirrers
- h. 75 µm screen
- i. Centrifuge
- j. Centrifuge bottles

Reagents:

- a. NaOH, 1M
- b. NaOH 0.001M

- c. Protease, Protex 6L, (Genencor Bacterial Alkaline Protease, Genencor International, Inc. Rochester, NY)
- d. HCL, 1M

Preparation of test samples:

Prepare sample of rice, preferably milled white rice grain

Isolation of starch:

- a) Clean- Wash and rinse 150 grams of rice with distilled water 2 times.
- b) Soak- Add 300 ml of distilled water and adjust pH to 8.0-8.5 with 1 M NaOH.
Monitor until pH becomes constant and soak the rice overnight.
- c) Wet grind- Discard supernatant and add 300 ml of 0.001 M NaOH. Blend approx. 50 grams of rice with the alkaline solution in a Waring blender at medium speed for 3 min. **Note:** rice becomes homogeneous liquid solution.
- d) Addition of enzyme – Add 500 ml of 0.001 M NaOH to the rice liquid and adjust pH to 9.5 with 1 M NaOH. Add Protese 10 ml.
- e) Incubation- Maintain pH at 9.5 and stir solution with magnetic stirring bar in a water bath at 40-45°C for 18h. (Constant monitor to not exceed below pH 8.5)
- f) Filtration- Filter the solution through a 75- μ m screen. Discard the overs (solids) retained on the screen.
- g) Centrifuge- Centrifuge the filtrate at 4000g for 20 min in 250 ml centrifuge bottles and discard yellow supernatant.
- h) Wash- Wash sediment with 50 ml of distilled water and centrifuge for 15 min.
Discard supernatant. Repeat twice.

- i) Adjust pH- Add 500 ml of water to the sediment and adjust pH to 6.5 with 1 M HCL.
- j) Purify – Centrifuge solution at 5000g for 20 min. Discard supernatant and remove upper dark tailing from starch sediment. Repeat several times to ensure complete removal.
- k) Dry- Allow sediment to dry in a convection oven at 40°C for 48 h. **Note:** Monitor to break apart big cake pieces to reduce drying time and prevent surface over-drying.
- l) Gently grind to fine powder and keep in dry, cool area for storage.

Appendix C

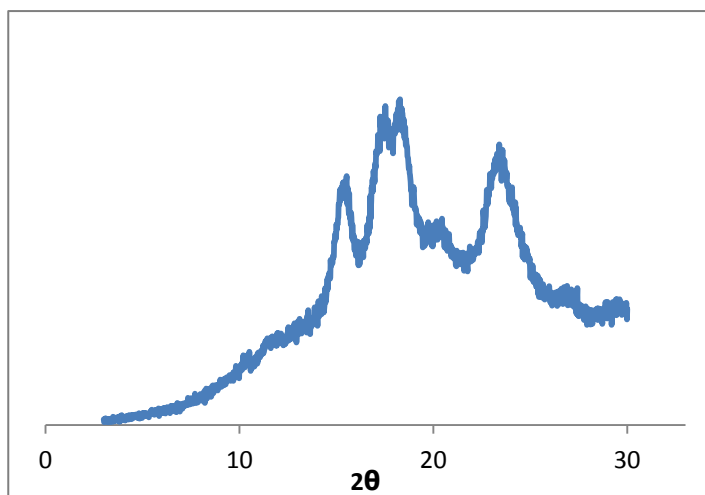
Detailed procedure for calculating starch relative crystallinity (Microsoft excel method)

Data requirements:

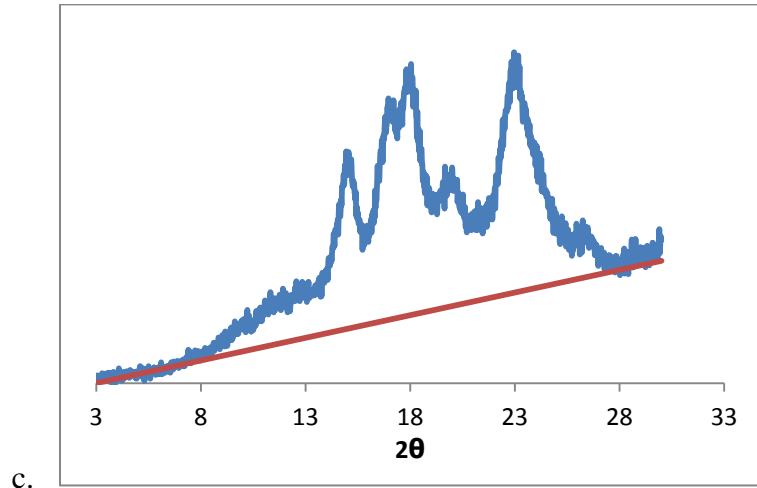
- a. X-ray raw data points in text or excel format

Procedure:

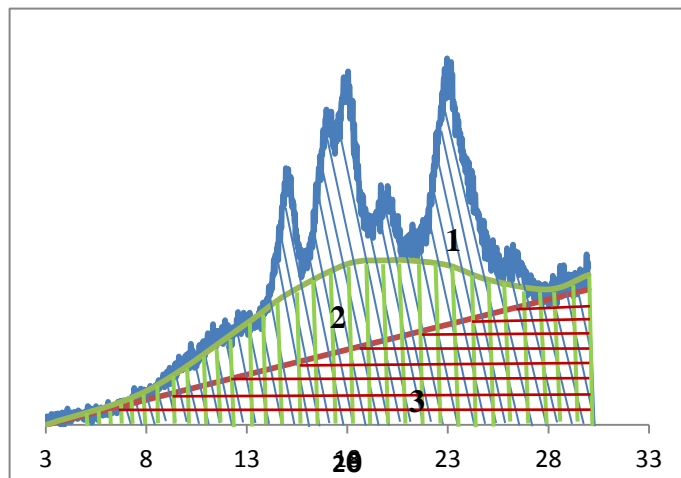
- a. **Create graph-** open raw data file in excel and create graph using X-Y scatter (sharp lines). Adjust line thickness to minimal.



- b. **Baseline-** Create a base line by plotting a linear line that would connect the first data point to the last data point. Adjust appropriately when line overlaps too little or too less into the curve.



- d. **Trendline**- Click “Add trendline” to raw data point. Select "polynomial" regression type. Choose the polynomial order ($n < 4$) which creates the most suitable curve fit for your graph. Check "display equation on chart". **Note:** A good trendline curve should fit raw data baseline and include the majority of peak area as shown in figure below



- e. **Plot curve**- Take the equation and insert raw data intensity values for “X” to get “Y” values.

- f. **Calculate graph area-** Use the “Y” coordinates to calculate area under the curve using the following equation. Repeat using the same equation for baseline (Area 3) and data point (Area 1).

$$\text{Area} = \Sigma((a_n + a_{n+1}) * h * 1/2)$$

Where

a_n = intensity (height of peak) of X_n

h = $X_{n+1} - X_n$

- g. **Calculate % Crystallinity (shaded area)**

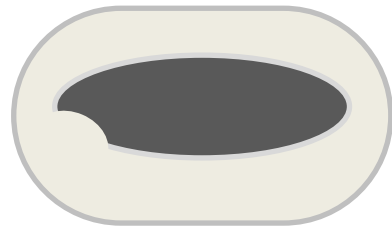
$$\% \text{ Crystallinity} = (((\text{Area 1} - \text{Area 3}) - (\text{Area 2} - \text{Area 3})) / \text{Area 1}) * 100$$

Note: If no suitable curve can be created using the trendline, an alternative method is to manually plugging in at least 10 data points to create a curve using the X-Y scatter (smooth lines) chart type.

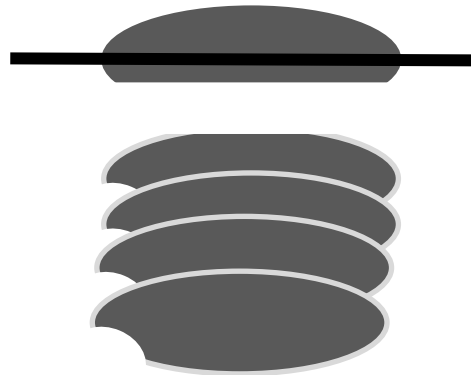
Appendix D

Cryosectioning

Dehulled fresh parboiled rice kernels were treated with cryoprotectant and submerged in cryomolds containing embedding medium and then were frozen in liquid nitrogen for 5 min. The sample mold was kept in the cryostat chamber at -20°C for 1 hour prior to sectioning. The mold was placed on the staged and longitudinal slices of the kernel were sectioned at $6\ \mu\text{m}$ thick with a stainless steel razor blade in a cryostat- microtome. Each section was transferred to a glass slide and fixed using a low temperature heating stage at low.



Embedded kernel



Longitude sections